J Bionic Eng 16 (2019) 967–993
DOI: https://doi.org/10.1007/s42235-019-0111-7

Journal of Bionic Engineering
http://www.springer.com/journal/42235

Design, Modeling, and Control of Biomimetic Fish Robot: A Review

Palmani Duraisamy, Rakesh Kumar Sidharthan, Manigandan Nagarajan Santhanakrishnan*

Robotics Laboratory, *Department of Electronics and Instrumentation Engineering*, *SASTRA Deemed University*, *Thanjavur*, *Tamil Nadu*-613401, *India*

Abstract

A comprehensive review on bio-inspired fish robots has been done in this article with an enhanced focus on swimming styles, actuators, hydrodynamics, kinematic-dynamic modeling, and controllers. Swimming styles such as body and/or caudal fin and median and/or paired fin and their variants are discussed in detail. Literature shows that most fish robots adapt carangiform in body and/or caudal fin type swimming as it gives significant thrust with a maximum speed of 3.7 $m \cdot s^{-1}$ in iSplash-II. Applications of smart or soft actuators to enhance real-time dynamics was studied from literature, and it was found that the robot built with polymer fiber composite material could reach a speed of 0.6 $m \cdot s^{-1}$. However, dynamic modeling is relatively complex, and material selection needs to be explored. The numerical and analytical methods in dynamic modeling have been investigated highlighting merits and demerits. Hydrodynamic parameter estimation through the data-driven model is widely used in offline, however online estimation of the same need to be explored. Classical controllers are frequently used for navigation and stabilization, which often encounters the linearization problem and hence, can be replaced with the state-of-the-art adaptive and intelligent controller. This article also summarizes the potential research gaps and future scopes.

Keywords: biomimetic fish robot, swimming modes, hydrodynamic modeling, motion control, smart actuators

1 Introduction

Biomimetic underwater vehicles have been an important area of research as it can replicate a real fish motion unlike propeller-based vehicles. Recent research on these vehicles explores various possibilities in improving propulsion efficiency, maneuverability and speed through different structural designs and control strategies[1–6]. The scientific study on fish locomotion[7–13] highlights the design structures, morphological features of fishes and mathematical modeling relating the complex motions with thrust and lateral forces. The first robotic fish (Robo Tuna) was developed in 1994 at the Massachusetts Institute of Technology with structures made of stainless steel, gears, and cables[14,15]. Subsequently, different models G9 series[16], Ichthus V5.7[17], iSplash-I[18] of robotic fishes were developed and tested. Recently in 2014 iSplash-II fish robot was designed and developed, which can travel with a forward velocity of 11.6 $BL \cdot s^{-1}$ (BL is body length of the fish) and in the standard unit, it is about 3.7 $m \cdot s^{-1}$[3]. This paper is organized into nine sections, and in each section, an attempt is made to identify the gaps, where further research can be carried out. Section **2** elaborates on different swimming styles of real fishes and implementation of the same into robotic fish. Section **3** focuses on classification of actuators used in fish-inspired propulsion system and its principle of working with significance. Modeling of hydrodynamics and its impact on swimming is essential for efficient design, sections **4** and **5** addresses the hydrodynamic effects and the challenges in modeling a robotic fish. Section **6** provides a detailed review of different control methods used in open and closed-loop environment. To understand the modeling in a better way, it is necessary to analyze and compare the performance parameters like forward velocity, undulation frequency, turning speed, impact on performance with respect to the number of joints. Section **7** analyses and compares these parameters from existing works and infers various solutions for further designs in this field. Section **8** provides a comprehensive discussion on various research gaps in robotic fish design, an outline for future directions in this field, and finally prospective conclusion.

The notable reviews in this field have been reported[19–26] time to time for the past two decades.

***Corresponding author:** Manigandan Nagarajan Santhanakrishnan
E-mail: manigandanns@eie.sastra.edu

Though, extensive review on swimming style has been found in literature, association of swimming style with various performance metrics are less investigated. This review paper presents a detailed comparison of performance metrics such as swimming speed *vs* body length, oscillation or undulation frequency, swimming style, actuator type, and joints. Additionally, swimming speed of real fish *vs* robot fish have been compared, which sheds light on further developments to be achieved in this area. A total of 23 robot fishes with electrical actuators and 20 with smart or soft actuators developed during the past 2 decades have been considered in this article. From the above comparison, the readers can identify the relative effects of various metrics and appropriately incorporate the same for achieving better design. Various conventional methods for kinematic and hydrodynamic modeling have been discussed with emphasis on its merits and demerits. The need for online data-driven modeling is highlighted since it can maintain the non-linearity thus minimizing the effect of linearization during control. With respect to control of fish robot, 14 manipulating variables and their impact on 5 control modes have been discussed. Application of classical and modern controllers in robot fish control with its limitations has been presented. The importance of intelligent controllers has been emphasized as the system model is highly non-linear and interaction between the system and surrounding is stochastic in nature. A total of 142 research articles and 10 books have been referred and Fig. 1 illustrates a bird's eye view on number of papers referred under the various sections.

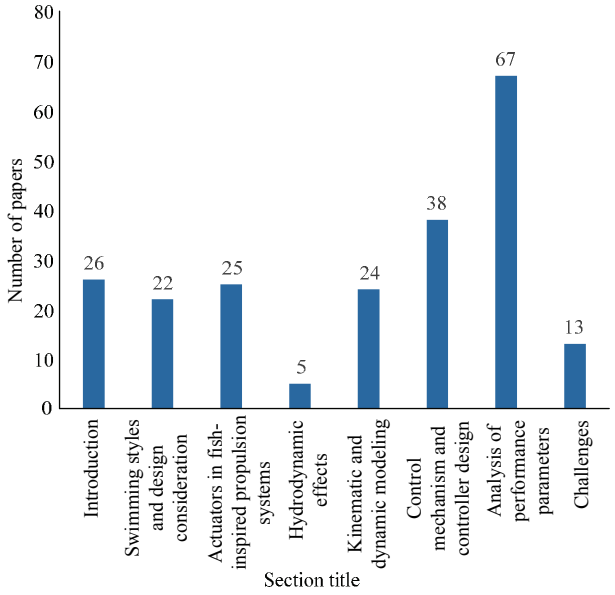

Fig. 1 Section-wise distribution of references.

2 Swimming styles and design considerations

Fish exhibits a mixture of movements, which involves both non-swimming characteristics such as jumping, gliding, crawling, *etc*. and swimming characteristics. The swimming movement can be classified as sustained and deciduous motion. The former involves traveling long distances at a constant speed, whereas deciduous motion is about quick begin and sharp turns to avoid being hunted. The current research areas are more inclined towards sustained motion compared to deciduous type. Fish swimming is basically categorized into two types based on propulsion such as BCF propulsion and MPF propulsion. BCF is also referred to as tail-flapping propulsion and exhibits rapid swimming and turning. Most agile fishes like Sailfish, Tuna, and Pike uses tail flapping. The MPF uses pectoral, dorsal, and anal fins to generate propulsion. Though this swimming mode is slower, it excels in terms of greater maneuverability with high Degrees of Freedom (DoF), enhanced controllability, and high efficiency.

About 85 % of the fish species produce thrust using BCF and the remaining 15 % with MPF propulsion[6]. The BCF type and MPF type propulsion are further categorized into two modes, such as undulation motion (Sine mode) and oscillation motion (C mode). Sine mode involves transit of full-wave along the body axis, whereas C mode involves oscillation of body or fins without exhibiting a wave formation. The classification of fish families based on various swimming styles discussed above is shown in Fig. 2. During steady movement, BCF type swimmer undergoes a traveling wave motion, where the fish body displaces laterally with respect to the body axis. This motion is also called as lateral motion denoted by $\boldsymbol{h}(x, t)$. Lateral motion is expressed using three odd Fourier terms as expressed in Eq. (1)[27]:

$$\boldsymbol{h}(x,t) = H(x)\sin(\omega t - \frac{2\pi}{\lambda}x), 0 \le x \le 1, \lambda \ge 0, \quad (1)$$

where, $H(x) = a_1 + a_2x + a_3x^2$ is wave envelope, a_1, a_2 and a_3 are amplitude coefficients, and $\lambda = 2\pi/k$. Increase of k (wavenumber) changes the swimming mode from C

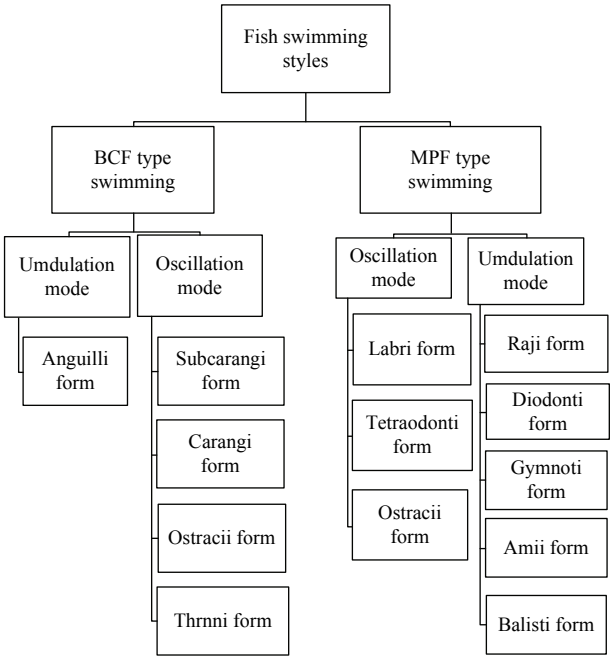

Fig. 2 Classification of fish families based on swimming styles.

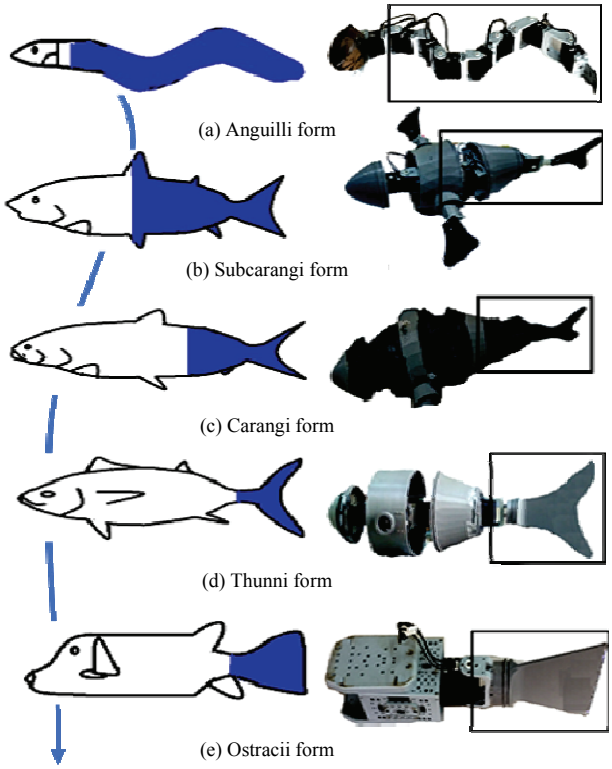

Fig. 3 Classification of BCF type swimmers highlighting the sections of its body that undergo flapping. The arrow mark indicates moving from undulation to oscillation mode (Adapted and redrawn from Ref. [29]).

to sine and x is the oscillation amplitude. An efficient mechanical design for fish robot can be achieved if the characteristics[28] of various fishes based on its swimming styles and modes are studied in detail. A short survey on the same has been done and presented below.

2.1 BCF type swimming

Based on the propulsion style, the BCF type is further categorized into undulation and oscillation mode. The sub-carangiform, carangiform, thunniform, and ostraciiform fall under oscillation mode category, whereas undulation mode includes anguilliform. The BCF type swimmer along with the section of its body, which undergoes undulation or oscillation is highlighted in Fig. 3. The prototype of each BCF swimming form is fabricated using 3-D printing technology, and it is also shown in Fig. 3. The propulsive force generated by both these modes incorporates two components, such as the lateral force and thrust force. The thrust force will act in the forward direction enabling the fish to move forward and lateral force act sideways resulting in significant energy loss as it induces yaw movement and sideslip.

In anguilliform, the whole body of the fish is involved in at least one body wavelength undulation and magnitude of undulation wave increases from head to tail. Here the energy loss due to lateral motion is significantly low, and additionally, it also possesses the ability to swim backward by changing the direction of undulation. The typical examples of anguilliform are Eel, lancelet, and Lamprey. This swimmer has high maneuverability, but low hydrodynamic efficiency as the undulation energy propagates all over the body leading to more energy loss.

The design of anguilliform robotic fish uses more servo motors to replicate snake-like motion. Though, it increases the maneuverability the power efficiency is significantly reduced. Instead of using servos, smart actuators (shape memory alloys) may be preferred, but it suffers from poor thrust generation. Anguilliform pattern locomotion in robotic fish was established by Niu *et al.*[30]. The work tries to build a robotic fish that replicate movements of real fish and swims backward by reversing the undulation pattern. Different works have been reported for locomotion pattern generation[31,32], modeling, and motion control[33] in anguilliform robots. Implementation of this form of locomotion in robotic fish

requires three to twenty serially linked actuators[23]. To confirm synchronization between the actuators, neural network-based approaches are mostly preferred, which models the serial actuators as a chain of coupled oscillators to replicate a real fish swimming pattern. It is identified that a phase lead between former link joint angle and latter link results in forward motion, phase lag leads to backward motion, and other variations result in turning motion. Based on the above identification, it is easier to generate a library for motion planning, which relates speed, turning radius with the joint angle, phase, and frequency[34].

In sub-carangiform and carangiform, the oscillation is confined to 1/2 and 1/3 of their body length respectively. The carangiform swimmer exhibits maximum swimming speed due to narrow peduncle and stiff caudal fin, which minimizes the lateral forces and enhances forward thrust. Jacks, snapper and mackerel fish belongs to the carangiform swimmers. Higher acceleration, velocity, and sweep characteristics can be achieved for S-shaped undulation, which can be generated using multi-link, planar tailed carangiform fish models[35]. Sub-carangiform swimmers have circular and rigid anterior part with regular geometrical shape caudal fin. Trout fish is an example for sub-carangiform swimmers. Sub-carangiform robots come with different designs such as flexible wire driven, shape memory alloys, and compliant links. Compared to anguilliform, it has higher speed but lower maneuverability with backward swimming capability[36].

Even today, the main challenge remains in hovering and turning characteristics of robotic fish. Suebsaiprom *et al.* designed six degrees of freedom 4-link carangiform robot[37] to move in a 3D space with improved maneuverability and trajectory tracking. Use of sliding mass and buoyancy tank ensures the stabilization and hovering. Researchers experimentally proved that flexible tail design with multiple joints and appropriate undulation frequency improved the forward thrust and swimming speed[38]. Xia *et al*. numerically proved the role of head swing in thrust generation[27]. They investigated that Tuna-like fish robot with spline head and body had improved hydrodynamic performance, if the leading and trailing edge amplitudes are properly chosen to be 0.05 BL and 0.08 BL respectively. In thunniform, the oscillation is confined to less than 30 % of BL, and the remaining portion of the body remains stationary (it does not participate in undulation). The lateral forces are compensated by stiff caudal fin and its streamlined body structure. It remains efficient in high-speed swimming but performs poorly at slow speed, higher accelerations & turning maneuvers. Typical thunniform swimmers (tuna, teleost, some sharks and marine mammals) have oscillating narrow peduncle and lunate type caudal fin. RoboTuna a robotic fish designed by MIT falls under this thunniform category. Ostraciiform swimmers are purely oscillatory type. It can be categorized into BCF or MPF styles based on the area of flapping[39]. During swimming, their body part remains stationary making it hydrodynamically less efficient[6,29].

2.2 MPF type swimming

MPF type swimmers are generally low-speed swimmers with velocity below 3 $BL \cdot s^{-1}$. The undulating fins are used by these fishes for propulsion, and these fins also provide a significant contribution in stabilization and maneuvering. Unlike in many robotic fishes, where the fins are assumed to be functional plates, the fins are highly complex in structure. This makes the maneuvering highly challenging in a robotic fish. The primary fin structure and its placement in bluegill sunfish are shown in Fig. 4. MPF type swimming is classified into undulation and oscillation types with rajiform, diodontiform, amiiform, gymnotiform, balistiform in former and labriform, tetraodontiform, ostraciiform in later. To understand the various types of MPF style swimmer, the body part that is involved in flapping is shown in Fig. 5.

Rajiform mode involves undulation of pectoral fins

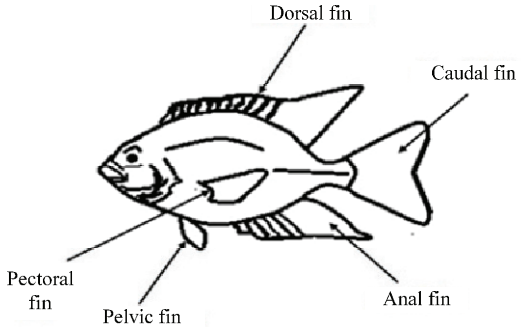

Fig. 4 Types of fins in Bluegill Sunfish[40].

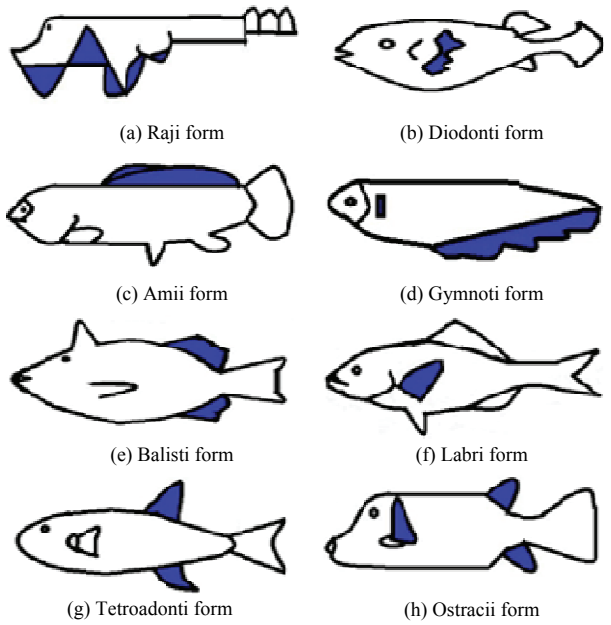

Fig. 5 MPF type swimming styles. Highlighted parts indicate where the flapping occurs (Adapted and redrawn from Ref. [22]).

with the amplitude of undulation higher in the apex of an anterior part of the fin and decays towards the posterior part combined with flapping in a lateral direction. The species such as Mantas, Skates, and Rays come under this category. Diodontiform mode also includes undulation of large pectoral fins but with at least two full wavelengths. In amiiform and gymnotiform mode fishes, the dorsal and anal fin undergoes undulation respectively, and it extends till the posterior part. Balistiform mode swimming found in triggerfish, which has a flat body and inclined median fins, combines both anal and dorsal fin undulation for propulsion. The oscillation in MPF type swimmer involves oscillation of median or paired fins. Ocean Sunfish are the best example for tetraodontiform mode, where the dorsal and anal fin combines as one unit to produce oscillation. Teleost fish in labriform mode undergoes two types of movements with pectoral fin oscillation. One movement is drag-based, which is efficient in slow speed and the other one lift based, and it is efficient in high speed[41].

Scientists have worked on MPF style based robotic fishes, where fins play a significant role in linear motion, turning, stability control, and hovering[42,43]. Many fish robot designs involve paired pectoral fin structure to increase propulsion efficiency and maneuverability. Fins can be actuated using any of the following methods such as rowing, feathering, and flapping. The rigid connection of pectoral fins with actuators, asymmetrical actuation of paired fins, slow recovery stroke, or higher beat frequency for longer joints will significantly reduce the propulsion efficiency. Behbahani *et al*.[42] observed improved thrust in the fish robot with flexible joints for pectoral fins and rowing type motion. Implementing a passive reverse stroke with variable drag area enhanced mechanical efficiency as well. Hence, it is summarized that flexible pectoral fins outperform in locomotion and mechanical efficiency, whereas rigid fins are effective for high fin-beat frequencies. To maximize the performance in terms of speed the fin's optimal power to recovery stroke speed ratio should be maintained in the range of 2–3[44]. Every fish species has a unique propulsion mechanism for locomotion. Researchers try to combine more than one mechanism in a single fish robot to improve efficiency. Zhang *et al*.[43] and Guo *et al*.[45] developed a fish robot with a coordination mechanism between two flapping pectoral fins and two caudal fins, which displayed a significant improvement in locomotion performance. Rhythm needs to be maintained between the movements of fin actuators to attain maximum efficiency. Central Pattern Generator (CPG) is a mechanism to generate different undulation or oscillation pattern in a rhythmic fashion for attaining agility and greater maneuverability. By properly tuning the CPG, a maximum swimming speed of 1.21 $BL \cdot s^{-1}$ was achieved even with low power servo motors[43].

3 Actuators in fish-inspired propulsion systems

It is important to design a bionic robot as smooth as a natural organism to achieve similar biological movements with higher efficiency and performance. Muscle like structures are essential for mimicking a real fish motion in the robot fish. Muscles of fish perform various operations like motor, spring, brake, and strut. It is challenging to duplicate all of these functions into the robot fish. The type of actuators used in robot fish typically falls into any one of the three categories shown in Fig. 6. Electrical actuators are widely adopted in many underwater vehicles and are simple in design, high operating speed, and readily available in market[26]. DC motors and servo motors are the two major variants used

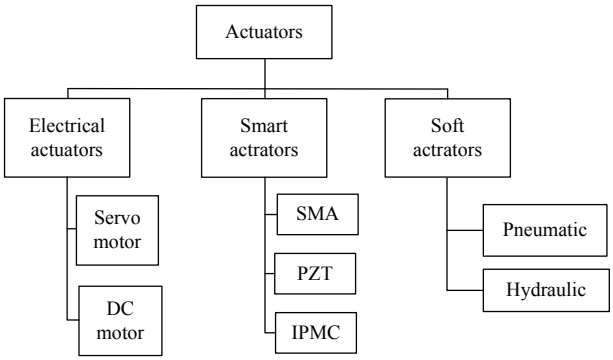

Fig. 6 Classification of actuators used in robot fish.

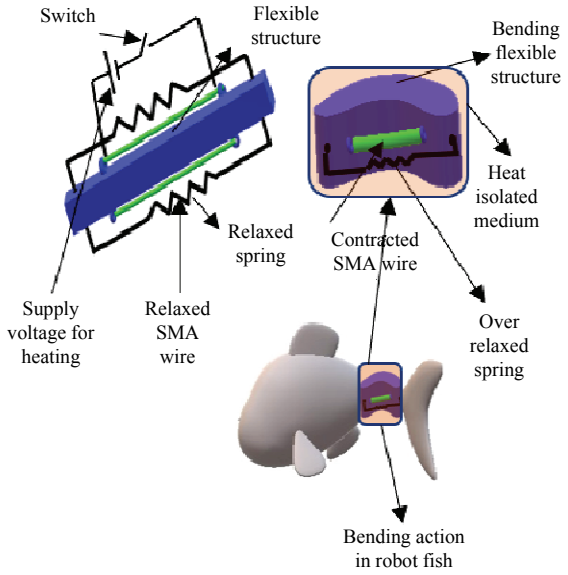

Fig. 7 Principle of SMA bending motion using flexible structure running parallel to SMA wire and spring.

under this category. Using transmission elements like gears, bearings, and harmonic drives, the desired actuation pattern, speed, and torque characteristics are maintained. Due to these translational elements, the system occupies larger space leading to higher drag force. Additionally, use of rigid bodies with electrical actuators for the development of robot fish needs lot of improvements to duplicate muscle-like actuation. Researchers are also focusing on smart actuators, which have the ability to perform complex motions similar to biological species. This mechanism is continuous, simple, and more robust than the discrete and rigid body motions present in electrical actuators. Smart actuators are fabricated with material heterogeneity; therefore, its dynamic response mimics desired body motions. The materials used for this mechanism may fall into three major categories, (i) Shape Memory Alloys (SMA), (ii) electroactive polymers (EAP), (iii) Piezoelectric Fiber Composite (PFC). Another simple and powerful technique used for underwater actuation is soft actuators, which is different from smart actuators in the sense of interacting mediums. The interaction of two different mediums (flexible structure with compressed air or pressurized fluid) produces bending motion whereas, in smart actuators, the applied electrical trigger causes a physical reaction to deform the structures in desired direction. The actuation principle implemented in robot fishes, and the limitations of smart and soft actuators are explained in detail as follows.

The SMA wires have the ability to act as an actuator element for bionic robot fish. It does not have translational elements like bearings and gears for actuation. Here, the propulsive structure of robot is divided into N segments. Each segment is made up of flexible structure united by SMA wires, as shown in Fig. 7. Heating this wire results in contraction of the same, which creates a bending motion on the flexible structure. Use of such continuous multi-segment structure along the whole body of the robot helps in bending motion of the entire robot fish body. The flexible polycarbonate structure with SMA wire is utilized for robot fish design. The bending motion reached a maximum of 38˚ at 90 ˚C with the nominal cooling time of 1.7 s and operating frequency of less than 1 Hz[46]. The SMA actuation employed in starfish robot used a Smart Modular Structure (SMS) and achieved a forward swimming speed of 0.07 $m \cdot s^{-1}$ at 1 Hz frequency[47]. Wang *et al.* developed a flexible biomimetic fin using SMA wire and implemented the same on a micro-fish robot. The robot was capable of swimming straight, and exhibited a turning motion with a maximum speed of 0.112 $m \cdot s^{-1}$ at 2.5 Hz oscillation frequency. Further, bending angle greater than 90˚ was obtained on both sides with respect to body axis[48]. SMA materials have low operating frequency and are only suitable for undulation motion-based fish robots. Recent advancements in this field proved that high-frequency actuation is also possible in SMA actuators with frequency up to 35 Hz[49]. This high-frequency oscillation can result in larger swimming speed and better maneuverability. However, this actuation is based on temperature change and robust control

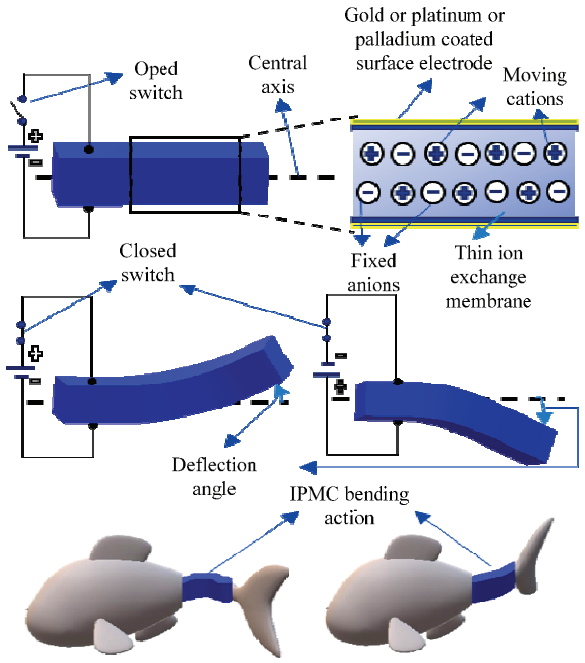

Fig. 8 Working principle of IPMC actuation (Adapted and redrawn from Ref. [55]).

of temperature in an underwater environment is highly challenging.

EAP materials can act as artificial muscles and has found greater interest in aquatic robots to produce significant bending deformations under low voltages. These materials are classified into Ionic Polymer-Metal Composite (IPMC) and conjugated polymers. IPMC based EAP material has been widely employed[50–54] in underwater actuation due to its compliance, lightweight, agility, and most importantly, lesser driving voltage (< 5 V). The working principle of IPMC actuation is illustrated in Fig. 8. The voltage excitation results in deformation of the material due to movement of cations towards the anode. Mechanical bending of the material generates a small potential difference between the electrodes, which makes this material useful for sensing as well, which is beyond the scope of this article. The IPMC based actuation can be used for propulsion of different parts of a robot fish and predominantly in caudal fin as it plays a vital role in swimming. Using IPMC materials, both BCF[36,52,54–57] and MPF[46,50,54,58,59] based swimming styles have been implemented. The swimming speed of the fish robot using IPMC material is less due to its low deflection angle, oscillation frequency, torque, and smaller body length. Initially, IPMC material was used as an electrolysis generator to produce hydrogen and oxygen gases from water. This phenomenon was used for depth control in an underwater vehicle. An experiment was conducted using artificial chamber, which includes the IPMC electrolysis generator and solenoid valve. IPMC actuation produces gases, which are stored in the artificial chamber and the volume of gas was controlled by a solenoid valve. The artificial chamber structure can reach a depth of 0.9 m in 4.7 s and returns back to the surface in 185 s[60]. Hence, IPMC material can simultaneously act as an underwater actuator as well as buoyancy controller.

Frequently used PFC material for actuation is lead-zirconate-titanate (PZT) composite. Flexibility, better angular deflection, and good electromechanical decoupling feature make these composites to be preferred for underwater actuation. The actuation principle is based on the inverse piezoelectric effect, which results in structural deformation on electrical excitation, and is used for flapping. Macro Fiber Composite (MFC) is a typical PFC material utilized for underwater propulsion. The Carbon-Fiber Reinforcement Polymer (CFRP), which is a thin elastic plate and when sandwiched between two MFC plates excited by larger potential produces mechanical vibrations on the CFRP plate. The applied potential ranges from −500 V to 1500 V and it produces a displacement of 40 mm in the caudal fin tip with 3 Hz flapping frequency. With S-shape bending deformation in the structure, a maximum swimming velocity of 0.6 $m \cdot s^{-1}$ was achieved[61]. PZT composites requires a larger driving potential (> 100 V) for actuation and hence, found less usage for underwater applications. But, IPMC and PZT materials have larger operating frequency range, which is suitable for both oscillation and undulation motions[25].

Pressurized fluids or compressed air can also be used for powerful actuation in robots, which is often called as soft robotics. A real-time implementation of this was done by Massachusetts Institute of Technology for underwater life exploration using a three dimensionally maneuverable and acoustic controlled robot fish. The powerful hydraulic actuation with remote-controlled commands can move the robot vertically up to 18 m in the oceanic field[62]. This was a major breakthrough in the field of bio-mimetic robotics for

underwater applications. Pneumatic control actuation is also preferred for soft robotics, which uses compressed air passing through a flexible and deformable structures to create continuous propulsive locomotion[63]. However, it requires higher energy batteries to handle compressed air valves and an extra storage unit for deflated air. The deflated air may also be released in the environment, which may have a significant effect in the overall buoyancy force acting on fish robot.

Miniaturized form of actuation is also found in the literature, which has a significant contribution to the development of underwater actuation systems. For example, an electrostatic film motor consists of two flexible Printed-Circuit-Boards (PCBs) arranged in such a way that the sliding unit can move on the stator unit to produce linear motion, which is attached to the caudal fin to produce flapping motion[64]. It is like a synchronous motor excited by six-phase AC supply. Two-phase AC excitation for sliding unit and four-phase AC for stator excitation. AC voltage of 2 kV (peak to peak) was used for excitation with the stator frequency of 500 Hz and 500 Hz ± 25 Hz for sliding unit, which results in 4 mm displacement. Using this, two models were developed, namely Seidengyo-I and Seidengyo-II, which achieved a forward swimming speed of 0.018 $m \cdot s^{-1}$ and 0.04 $m \cdot s^{-1}$ respectively[64]. Bonnet *et al.* developed a compact size (63 mm), single board, zebrafish inspired miniaturized robot for behavioral study of living fish. This work uses rigid-flex PCB design to provide flexibility in the control board resulting in reduced system volume. Stimuli light waves are generated from robot fish using flashing LEDs, which attracts the living zebrafishes thus helping in real-time behavioral study. Structural similarity helps the robot in camouflaging a living fish so that closer observation is possible[65]. Depth motion was also achieved through magnetically coupled mobile robot moving under a circular aquarium[66]. Takada *et al.* developed a miniaturized fuel cell powered robot, which is first of its kind. A polymer electrolyte fuel cell often referred as power tube was designed and developed for energy efficient locomotion. The power tubes act like an alkaline cell, which requires hydrogen as fuel. The calcium pack present in the robot fish reacts with the surrounding water to generate the required hydrogen. Due to polymer electrolyte fuel cell, size and weight of the robot is reduced helping in long distance swimming. Using floating power tube system with magnetic actuation, the robot fish can be moved vertically to achieve 3-D maneuverability[67].

4 Hydrodynamic effects

Water properties play a crucial role in the swimming characteristics of any fish. The density of water reduces the effect of gravitational force on the fish and hence body size of the fish does not affect its propulsion to a larger extent. Assuming water to be an incompressible fluid, there is an exchange of momentum from the fish body to water and vice versa during swimming action. This momentum transferred from water to fish body surface introduces a thrust on the fish resulting in motion. Hence, it is very important to understand the dynamics and properties of water. Density and viscosity are unique properties of water, which is highly sensitive to temperature and salinity. Density has a positive coefficient with respect to temperature and negative coefficient to salinity. Viscosity has a negative coefficient with respect to both temperature and salinity. The ratio between dynamic viscosity and density is termed as kinematic viscosity. These parameters decide the Reynolds number (*Re*) described by Eq. (2) and are used to calculate relative magnitudes of inertial and frictional forces in any hydrodynamic environment[9].

$$Re = \boldsymbol{u} L \rho_{\omega} \mu^{-1}, \tag{2}$$

where, $\boldsymbol{u}$ is velocity, L length of robotic fishtail, ρ_{ω} density of water, and μ viscosity of water. For low values of *Re*, sink, buoyancy and weight forces are dominant, and if *Re* is high, the horizontal thrust and drag forces are dominant. The ranges of *Re* is less than one for protozoa, amoeboid, and other related species, whereas in the order of 10^8 for blue whale[8,9]. Carangiform swimmer type has the Reynolds number around 10^6, and for anguilliform, it is around 10^4[68]. The dominant forces acting on a fish are categorized into vertical and horizontal forces, as shown in Fig. 9. The horizontal forces include drag (D), thrust force (T) generated by tail flapping, and vertical force includes upward forces due to buoyancy (A), tilted pectoral fins (B), asymmetry in tail shape (C) and downward force (W) due to the weight of the fish. The buoyancy force $\boldsymbol{F}_b$ can be written as:

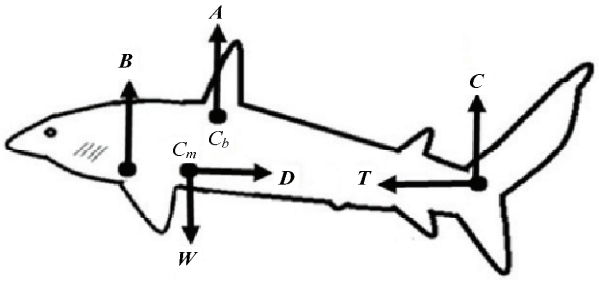

Fig. 9 Various forces acting on a Shark fish at rest (Adapted and redrawn from Ref. [10]).

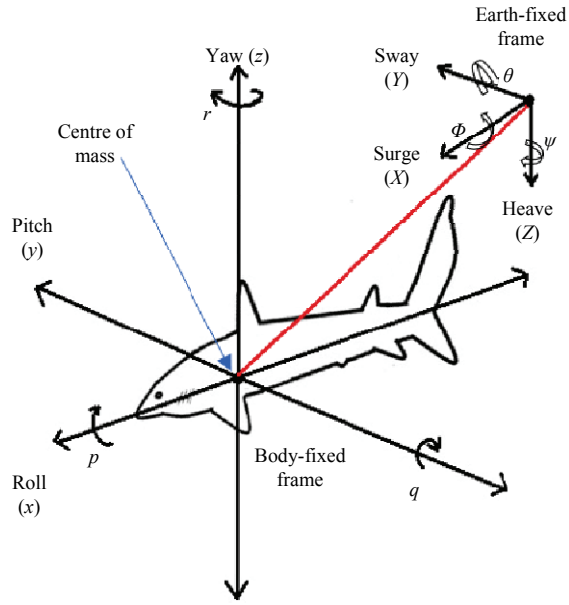

Fig. 10 Description of fish body in space and assigning frame for roll, pitch, and yaw motions (Adapted and redrawn from Ref. [37]).

$$\boldsymbol{F}_b = V\rho_\omega g, \tag{3}$$

and weight of the fish W as:

$$W = V\rho_a g, \tag{4}$$

where, V is the volume of robotic fish, g is acceleration due to gravity, ρ_ω is the density of water and ρ_a the average density of fish. The distribution of weight along the body of fish, determines the position of buoyancy force and the corresponding densities decide the position of weight force. The sum of static and dynamic pressure as given in Eq. (5) remains constant under a steady flow of water without swirl. The dynamic pressure is generated due to the interaction of fluid particles:

$$\frac{1}{2}\rho_\omega \boldsymbol{u}^2 + P = \text{constant}. \tag{5}$$

Due to tail movement, the water particle close to fish body moves with the speed of fish ($\boldsymbol{u}$). The overall drag force ($\boldsymbol{D}$) on the fish due to skin friction is proportional to dynamic pressure and body surface area of the fish and is given by Eq. (6).

$$\boldsymbol{D} = \frac{1}{2}\rho_\omega \boldsymbol{u}^2 A_w C_{dw}, \tag{6}$$

where, C_{dw} is the drag coefficient, and A_w is the body surface area of the fish. According to Ellington[38,69], drag force can be related to the frontal area of fish and is given by:

$$\boldsymbol{D} = \frac{1}{2}\rho_\omega \boldsymbol{u}^2 A_f C_{df}, \tag{7}$$

where, A_f is frontal area of fish and C_{df} is drag coefficient of frontal area of the fish. Underwater vehicles like fish robot require the clear knowledge of drag force parameters to analyze the dynamics which assists hydrodynamic modeling and energy efficiency of the fish robot. For motion modeling, the displacement with respect to global coordinates X, Y, and Z are specified by the surge, sway, heave, and θ, ϕ, ψ are its corresponding rotational angles. To represent the orientation of a fish body, body-fixed frame coordinates are described as roll, pitch, yaw respectively, and p, q, r represent its rotational angles[37] as shown in Fig. 10.

5 Kinematic and dynamic model

5.1 Kinematic modeling

Kinematics is the study of motion related to any robotic system without relating the forces/torques that cause it. Usually, a robotic fish consists of rigid bodies united by joints. The location and orientation of the rigid bodies in space together are termed as the pose. The kinematics elucidates the pose, speed, acceleration, and all higher-order derivatives of pose that comprise a mechanism of motion. The simplest way to model the kinematics of the robotic fish is using homogeneous transformation. Robotic fish is considered to be a serial link planar manipulator. The tail tip coordinate frame is related to the head coordinate frame by using a series of translational and rotational operation as described by Euler angle representation[70]. Mostly inverse kinematic solutions are preferred for modeling, which predicts the joint angles from known tail tip position. The robots

with rigid body exhibit lower efficiency compared to flexible caudal fin structure[71,72]. This flexibility enables the robot to generate maximum thrust for every incremental actuation. Resonance in the structure is identified, and the actuation can be tuned to achieve maximum thrust efficiency. The behavior of flexible caudal fin system is complex to model because of its jointless framework. Bernoulli-Euler beam equation is utilized for modeling such a compliant tail in robotic fish kinematics[73–75]. The force generated along the lateral direction[76] by a differential element on the flexible tail is given by:

$$[\boldsymbol{Q}(x,t)+\frac{\partial \boldsymbol{Q}(x,t)}{\partial x}\mathrm{d}x]-\boldsymbol{Q}(x,t)+\boldsymbol{f}(x,t)\mathrm{d}x = m(x)\mathrm{d}x\frac{\partial^2 \boldsymbol{y}(x,t)}{\partial t^2}, 0<x<L, \tag{8}$$

where $\boldsymbol{Q}(x, t)$ is a shearing force, $\boldsymbol{f}(x, t)$ is transverse force per unit length caused by shearing force, $\boldsymbol{y}(x, t)$ is transverse displacement, $m(x)$ is mass per unit length and L denotes tail length. The effect of shear force deformation can be ignored because this distortion is small compared to bending deformation; Ref. [76] for further details. The main drawback of this model is that it becomes non-linear if the flapping magnitude is large. This theory is valid only if the compliant tail length to thickness ratio is greater than 10. Yu *et al.*[77] have discussed on kinetic model of drift-less unicycle vehicle which comprised of two independent actuators connected on common axle whose direction was rigidly linked to the robot chassis. For unicycle type robot the kinematic model equation is expressed as:

$$\begin{pmatrix}\dot{\boldsymbol{x}}(t)\\ \dot{\boldsymbol{y}}(t)\\ \dot{\boldsymbol{\theta}}(t)\end{pmatrix}=\begin{pmatrix}\boldsymbol{v}(t)\cos\theta(t)\\ \boldsymbol{v}(t)\sin\theta(t)\\ \boldsymbol{\omega}(t)\end{pmatrix}, \tag{9}$$

where, (x, y) is position variables in the cartesian coordinate system, θ denotes the direction, $\boldsymbol{v}(t)$, $\boldsymbol{\omega}(t)$ represent the linear and angular velocity of fish robot. This model cannot be asymptotically stabilized at a preferred posture using continuous feedback[78], hence, resulting in overall instability.

The commonly adopted kinematic model of a multi-link robotic fish is in the form of sinusoidal body wave called as Lighthill's traveling wave equation, or traveling wave equation[36,79,80], which given by Eq. (10):

$$\boldsymbol{y}(x,t)=(A_1x+A_2x^2)\sin(\beta x+\omega t), \tag{10}$$

where, y is the transverse (side) displacement of the fish body, A_1 is the linear wave amplitude envelope, A_2 is the quadratic wave amplitude envelope, x is the displacement along head to tail axis (forward), β indicates the wave number ($\beta = 2\pi/\lambda$), λ the body wavelength, and ω body wave frequency. In order to assure head stability in robotic fish modified Lighthill's body wave equation[81] was proposed as:

$$\tilde{y}(x,t)=(A_1x+A_2x^2)\sin(\beta x-\omega t)+A_3A_1x\sin\omega t, \tag{11}$$

where, A_3 is scaling factor used to vary the magnitude of body wave.

Lighthill[82,83] formulated the fish motion as traveling wave displacement vector $\boldsymbol{h}(x, t)$:

$$\boldsymbol{h}(x,t)=f(x)g(t-\frac{x}{c}), \tag{12}$$

where, $f(x)$ represents the magnitude term, $g(x)$ represents frequency dependent wave function, and c represents the body velocity. Lighthills' slender body theory[82] includes the lateral displacement in undulatory propulsion, which is given by:

$$\boldsymbol{V}(x,t)=(\frac{\partial \boldsymbol{h}}{\partial t})+\boldsymbol{u}(\frac{\partial \boldsymbol{h}}{\partial x}). \tag{13}$$

5.2 Dynamic modeling

Dynamic modeling is the study of motion, which relates contact forces with actuation and acceleration with motion trajectory. The general equation of motion can be written as:

$$\boldsymbol{T}-\boldsymbol{D}=M\boldsymbol{a}, \tag{14}$$

where, $\boldsymbol{T}$ is the forward thrust force, $\boldsymbol{D}$ is the drag force due to body friction of the robotic fish and hydrodynamic properties, M is mass of the fish, and $\boldsymbol{a}$ is acceleration. The dynamic motion equation of fish robot obtained using Lagrange-Euler formulation is given by:

$$\frac{\mathrm{d}}{\mathrm{d}t}(\frac{\partial \mathcal{L}}{\partial \dot{\boldsymbol{q}}_i})-\frac{\partial \mathcal{L}}{\partial q_i}=\tau_i, i=1,2,...,n. \tag{15}$$

The Lagrange function ($\mathcal{L}$) is expressed as the difference between kinetic (K_E) and potential energy

(P_E), $\boldsymbol{q}_i$ is the joint variable of ith coordinate, and τ_i is the generalized force at ith joint acting on the head.

$$\mathcal{L} = K_E - P_E. \tag{16}$$

For dynamic modeling, it is assumed that the fish robot consists of rigid links united by joints same as a serial link manipulator. The equivalent model of the fish robot in a body-fixed frame coordinate system is shown in Fig. 11. The Lagrange-Euler dynamic formulation for link-i of the equivalent model is:

$$\boldsymbol{M}(\boldsymbol{\theta}_i)\ddot{\boldsymbol{\theta}}_i + \boldsymbol{C}(\boldsymbol{\theta}_i, \dot{\boldsymbol{\theta}}_i)\dot{\boldsymbol{\theta}}_i^2 + \boldsymbol{B}\dot{\boldsymbol{\theta}}_i + \boldsymbol{K}\boldsymbol{\theta}_i = \boldsymbol{F}_i, \tag{17}$$

where, $\boldsymbol{M}(\boldsymbol{\theta}_i)$ is inertia coefficient, $\boldsymbol{C}(\boldsymbol{\theta}_i, \dot{\boldsymbol{\theta}}_i)$ is Coriolis force coefficient, $\boldsymbol{B}$ is damping coefficient, $\boldsymbol{K}$ is spring constant, $\boldsymbol{F}_i$ is force on link-i including hydrodynamic forces, and $\boldsymbol{\theta}_i$ is angle between the successive links[37]. The dynamic modeling of robotic fish involves two stages, as shown in Fig. 12 namely, hydrodynamic parameter identification and hydrodynamic modeling. The main challenge lies in modeling the hydrodynamics. Currently, researchers follow two methods to model the same, namely numerical and analytical methods. Numerical methods are systematic in approach but arduous as it necessitates solving complex Navier-Stokes equations[84], whereas analytical methods are direct and realistic. The numerical approaches for hydrodynamic modeling are summarized in Table 1 with pros and cons. Various analytical methods and their significance are listed in Table 2. They adopt the resistive theory[89], waving plate theory[90], and Lighthill's theory[11–13]. It is evident that Lighthill's theory is more practical and hence, frequently used for hydrodynamic modeling. Two extended versions of Lighthill's theory, such as Lighthills' Elongated Body Theory (EBT)[12] and Large Amplitude Elongated Body Theory (LAEBT)[13] are also well suited for robotic fish modeling in a dynamic environment. Reactive theory-based EBT[12] is the preferable choice for high-speed carangiform propulsion system, and LAEBT combines resistive and reactive theory for modeling the deformed tail body[13].

Another important part in dynamic modeling is identifying hydrodynamic parameters like drag, lateral, and buoyancy forces. These parameters can be predicted from standard data, Computational Fluid Dynamics (CFD) simulation, experimental measurements, and

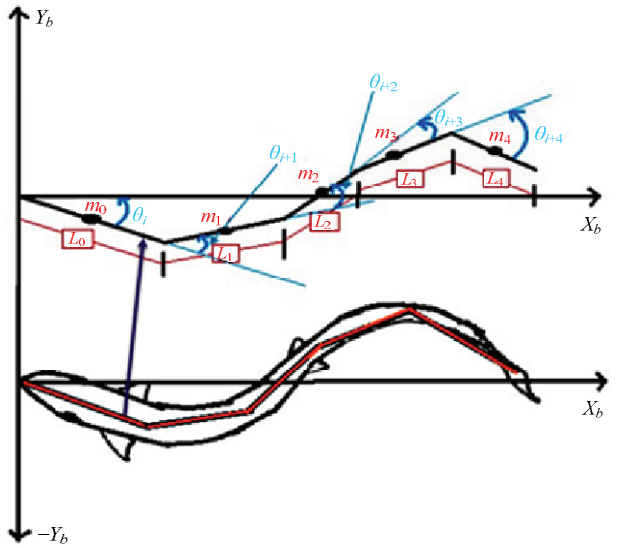

Fig. 11 Equivalent model of fish robot in body-fixed frame coordinate system, where $L_0 - L_4$ represent link lengths from head to tail, $m_0 - m_4$ represent the center of mass of links $L_0 - L_4$ and θ_i is the angle between the successive links.

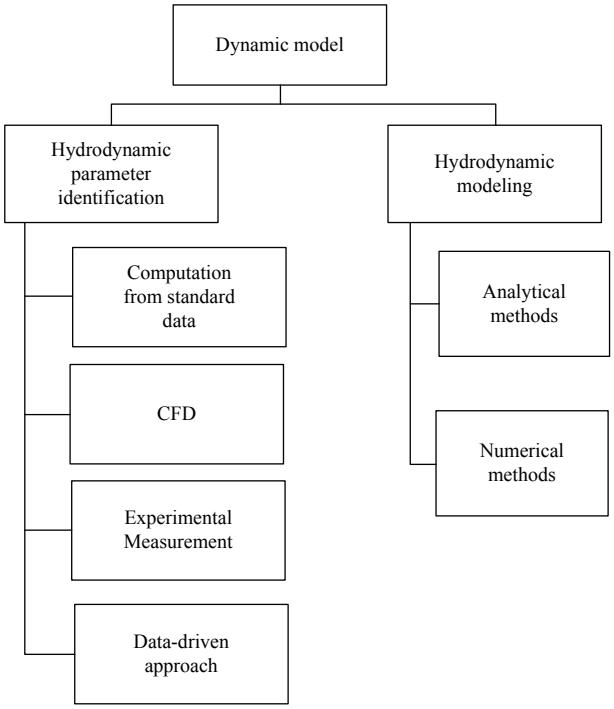

Fig. 12 Stages in dynamic modeling of robotic fish.

real-time data analysis (data-driven model approach)[70]. Prediction from standard data is suitable only for known shapes and environmental conditions. CFD provides a qualitative prediction of fluid flow using mathematical modeling, numerical methods, and software tools through simulations. Phase lag during undulation of fins,

Table 1 Numerical methods used for hydrodynamic modeling with its pros and cons

Numerical methods	Pros & Cons
Newton–Euler formulation[81]	1. Computationally simple 2. More intuitive 3. This method is based on the principle of force balancing 4. Futile computations particularly in closed chain dynamics
Kane's method[85]	Computationally efficient method for closed-loop systems with precise motion equations
Navier–Stokes equations[84]	Accurate but time-consuming
Lagrange method[86,87]	1. Energy based model which relates kinetic and potential energies of each link with resultant torque 2. Computationally complex
Morison equation and Strip method[70]	1. Simple and more intuitive 2. Directly relates velocity and acceleration with body motion 3. Not suitable for a body having larger dimensions with respect to wave height and not smaller compared to the incident wavelength[88]
Coupled dynamic model[73]	Distributed model, which couples rigid body dynamics with vibrating tail dynamics

Table 2 Analytical methods and their significance

Analytical methods	Significance
Resistive theory[89]	Fluid forces compose of longitudinal skin friction and lateral drag forces. Neglecting inertial forces remains the main drawback
Waving plate theory[90]	Models fish as undulating infinitesimal height 2-D plate, which is a theoretical one
Lighthill's theory[12,13,83]	Lighthill's theory describes the dynamic forces experienced by a fish in a horizontal plane and is widely used for dynamic modeling. The following are the advantages of the same. 1. Greater computational efficiency[80] 2. Easy to estimate the hydrodynamic parameters 3. Considered to be a standard motion model for robotic fish motion. 4. Lighthill's wave function with multi-degree of freedom generates different swimming patterns like carangiform, anguilliform, *etc*.,[82] Elongated Body Theory incorporates the effect of added mass[12] Large Amplitude Elongated Body Theory (LAEBT) best suits for giant deformations of the tail[13] LAEBT with Euler-Bernoulli theory models the deformation of flexible tail movement[91]
Airfoil theory[51,73]	1. Used for body and Fin surface modeling 2. Parameters for the medium of contact (air) is completely different

drag, and lift coefficients can be identified using the CFD tool for real-time modeling of robotic fish[92,93]. In the experimental approach, the gray box identification algorithm is used to build the setup for dynamic parameter identification. This algorithm does not encompass the entire dynamics of real-time water bodies, leading to inaccuracies[94,95].

Data-driven modeling is simple, and the hydrodynamic parameters can be captured using sensors mounted on the fish robot. Additionally, in real-time several hydrodynamic parameters are identified, and the controller needs to be tuned accordingly, which is really challenging, and thus giving an extra lead to a data-driven approach. This approach has been widely studied in ships and underwater propeller-based vehicles. Yu *et al*. developed data-driven modeling for a multi-joint fish robot with an irregular geometric profile[70]. More experimental trials should be conducted to capture the complete dynamics of the system in the data-driven approach, thus increasing the data size. The amount of thrust generated by the fish depends on the velocity and mass of the displaced water (added mass). Like in aerodynamics, where airfoil influences the vortices, in robotic fish, the tail acts as a hydrofoil to generate vortices. These vortices result in water particle movement along the fish body, thus inducing a thrust. According to Lighthill's theory, the thrust generated around the fish has three components, (a) reactive forward pushing force, (b) rate of change of momentum at the tip of tail blade and (c) rate of change of momentum due to the displaced mass of water. Dynamic modeling involves mathematical formulations based on application requirements. Nguyen *et al*. proposed a model using Kirchhoff's equation for motion with Euler-Bernoulli beam theory based vibrating

caudal fin model and Morison equation for hydrodynamic analysis. The instantaneous thrust generation in the tail tip was approximated using LAEBT[38]. Yuan *et al*. integrated hydrodynamic study by solving the Morrison equation and dynamic modeling based on Newton-Euler formulations. Finally, the state-space model relates a dynamic analysis to the head coordinate system. The thrust generated for one undulation is oscillatory in nature and hence, is averaged for one cycle and converted to the discrete domain for effective thrust control[70]. To derive the relationship between control input and thrust generation in the fish robot, the LAEBT mechanism was incorporated by Verma and Xu[96]. Most significantly, the thrust is modeled as a linear function of control input, so that affine-in control can be achieved. Inclusion of thrust delay in controller design improves the speed control performance considerably[97].

6 Control mechanism and controller design

This section describes various strategies of control and control parameters used in robotic fish. It also elaborates on generalized closed-loop control used in robotic fish to achieve desired navigation. Various controllers used in this field and the scope of other controllers in robotic fish are also discussed, which can provide a future direction in controller design.

6.1 Control strategies

Locomotion control employed in robotic fish can be classified into five categories namely, (i) direction control, (ii) depth control, (iii) speed control, (iv) stabilization and trajectory control. Different motion control mechanism addresses different control parameters to achieve desired motion in robotic fish and is summarized in Table 3. Direction control approach manipulates the robotic fish to create forward/backward and turning motions. Proper selection of amplitude, frequency, and phase angles of actuation promises the desired direction of motion. Forward motion is achieved by flapping the caudal fin in equal amplitude with respect to the body axis, as shown in Fig. 13. Selection of unequal actuation amplitudes with reference to body axis enables the fish robot to make a turn[35]. Pectoral fin flapping and head swing also play a significant role in direction control.

Depth control in a robotic fish is achieved through

Table 3 Summary of motion control parameters for different motion control strategies

Type of motion control	Control parameters
Direction control	Undulation amplitude, frequency and phase
Depth control	Pitch angle, position of center of gravity
Stability control	Pitch, yaw, and roll angles, buoyancy force
Speed control	Amplitude of undulation or oscillation, undulation pattern, flapping part length, frequency, thrust delay, and drag force
Trajectory control	Current pose, speed, and reference of guidance

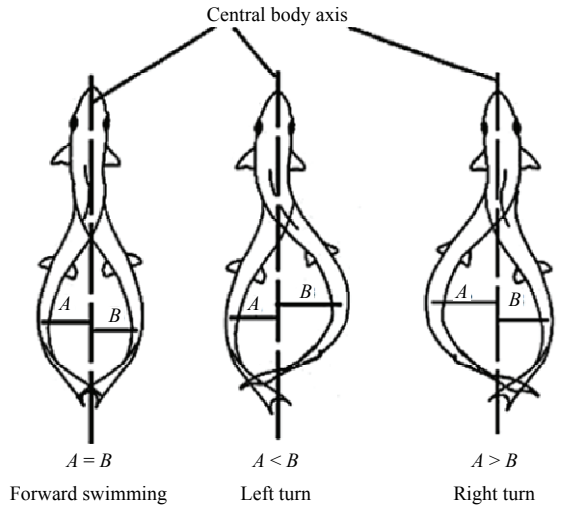

Fig. 13 Direction control mechanism in fish.

different techniques like ballistic tank approach, tilted pectoral fin arrangement, and sliding mass. Ballistic tank approach is a widely preferred choice, where robotic fish weight is altered by changing the volume of water in the tank. Vertical motion can be achieved by increasing the weight force until it exceeds the buoyancy force. In sliding mass control, the vertical motion is achieved by changing the center of gravity using movable masses. Adjusting the attack angle of pectoral fins to achieve depth control has also been investigated[81,98]. Here, depth control is closely related to the swimming velocity. During forward swimming, the angle of attack induces pitch angle variation and makes the robotic fish move up/down. Stability can be achieved by adjusting the pitch and roll angles of the fish robot. A four-tank balancing system for pitch and roll angle adjustment for robot stabilization is reported in Ref. [99], and it is a very slow process. A 1-DoF barycentre mechanism can adjust the center of gravity of the fish robot to maintain stability[100] in one direction. To achieve both pitch and

roll angle stabilization, a 2-DoF barycentre mechanism was implemented[101] using sliding mass control.

Speed control in robotic fish depends on several parameters like undulation amplitude, undulation part length, undulation pattern[35], frequency, *etc*. The literature illustrates the ease of frequency manipulation as compared to other identified parameters. Robotic fish velocity is affected by thrust gradient, thrust delay, and drag force[96], which has to be compensated to achieve the desired speed. From literature, it is seen that a top speed of 3.7 $m \cdot s^{-1}$ was achieved using a 4-joint carangiform robotic fish iSplash-II[3]. Trajectory control is naturally a closed-loop system involving both direction and depth control modes. It predicts the current status (position, orientation, and velocity) of the fish robot and control the same with respect to the reference trajectory. Straight and circular path 3-D trajectory tracking was investigated in simulation platform[37] with negligible tracking error using 6-DoF (heave, surge, sway, roll, pitch, and yaw) robot model.

6.2 Closed-loop control systems

Major objective of a robotic fish is to (i) mimic the real fish motion and (ii) track the reference trajectory or reference speed. The motion of real fish is fundamentally a sequential operation of caudal fin muscles. Two different approaches, namely kinematic based approach[3,82,102], and Central Pattern Generator (CPG)[103–107], has been widely employed in literature to achieve such sequential operations. Kinematic based control involves inverse kinematic fish model to generate the required joint angles and sequences. Increase in number of joints makes the inverse kinematic solution tedious. On the other hand, CPG control eliminates the need for an inverse kinematic solution to determine the individual joint position. It modulates the higher-level parameters like amplitude and frequency of the body wave equation based on the required pattern. Then, the body wave equation is discretized to generate required position of individual joints. CPG focuses on the generation of coordinated movements along the fish body, which is important to generate desired pattern for achieving enhanced thrust, velocity, and acceleration. It is well-suited for serial joint manipulator employed in an unstructured and dynamic environment. This makes CPG a preferred choice of

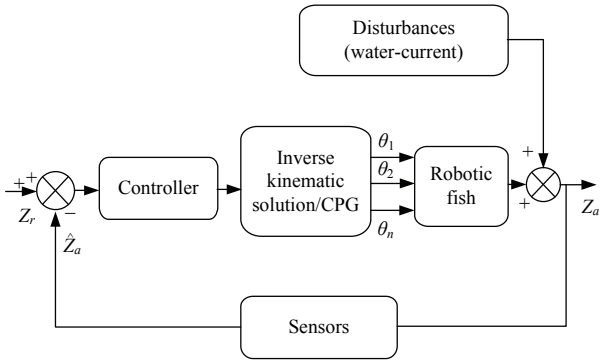

Fig. 14 Basic block diagram of the closed-loop control system in robotic fish.

actuation for robotic fish. However, it involves many uncertain parameters which are heuristically chosen for achieving better performance[36].

Several closed-loop control techniques[81,85,96,97,108,109] have been reported and the basic methodology adopted is shown in Fig. 14. Current position ($\hat{Z}_a$) of the robotic fish in a 3D space is determined by the Inertial Measurement Unit (IMU) and vision sensors. IMU integrates accelerometer and gyroscope data to determine the position and orientation, respectively. Due to poor visibility caused by turbidity & scattering effect[110–114], vision sensors are less employed for underwater robotic applications. To determine flapping motion of a robotic fish, the controller uses error between the target (Z_r) and the actual position predicted by the sensors. The signal generated by the controller describes the flapping angle, amplitude, phase, and frequency of body wave equation. Each joint position (θ_1 to θ_n) is controlled either by the inverse kinematic solution or CPG mechanism based on the generated body wave equation. Water current is a major source of perturbation in realizing the fish motion. Thus, the objective of the controller is to maintain sustained motion of each articulated joints for target tracking and stability maintenance.

Controllers employed in robotic fish can be categorized into three types, namely, (i) Classical, (ii) Intelligent and (iii) Hybrid control technique as illustrated in Fig. 15. Classical control involves the use of Proportional-Integral-Derivative) PID controller[73] to minimize the tracking error. Proportional controllers are used in guided swimming to control the orientation of robotic fish[115]. A passive approach using proportional controller-based locomotion employed for swimming along the

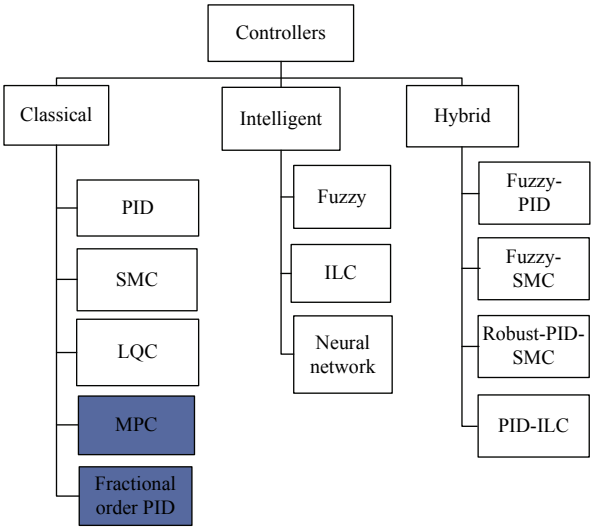

Fig. 15 Category of controllers used for robotic fish (*white box – indicates controllers implemented in the fish robot, grey box – indicate unimplemented controllers in robotic fish but have scope for investigation).

wall of a glass aquarium is investigated[86]. Pressure variation due to the wall in an aquatic environment is sensed using pressure sensors distributed along the head and body of robotic fish. Current distance and orientation of the robot with respect to the wall is identified from the ratio of pressure magnitude and its variation. Based on this ratio, a PID controller is employed to decide the further course of action for the robot to follow the wall closely. Image theory approach was utilized for measuring these pressure variations theoretically and verified through simulations as well as real-time studies. A good correlation was observed, and hence, it was recommended for coordination control in robotic fish[86]. Linear quadratic control and Sliding Mode Control (SMC) has received a lot of attention over recent years. SMC is capable of handling unstructured disturbances like water currents and can minimize the tracking error[96]. Model Predictive Control (MPC) and fractional order PID controller are highly successful techniques in controlling a serial link manipulator[78]. This brings in a lot of research scope in extending this MPC for robotic fish. Non-linear nature of robotic fish gives scope for investigating the application of fractional order PID controller in that area. Serial joints of the fish robot body can be considered as a cascaded system, and hence, the inverse model of the system can also be employed for control applications.

In intelligent control methods, fuzzy control is a powerful tool to handle uncertainties and non-linear dynamics, which makes it an ideal choice for motion control of robotic fish. Robustness of fuzzy logic systems can provide efficient depth control amidst poor image quality in underwater[81]. Control of depth and direction simultaneously is difficult to achieve. Hence, depth control is performed using a reference depth value of the artificial target initially, followed by direction control to reach the real target. In this study, the robotic fish uses spiral motion to reach the required depth. Other techniques involve the use of ballistic tanks, gliding motion, fins, sliding mass to make the fish robot dive in a 3D environment. Fuzzy control of paired pectoral fins[116] and heading control[117] to achieve desired motion has also been investigated, which outperforms in terms of maneuverability and stability. Machine learning techniques are found to be an ideal tool for fish robot modeling with affine in control. The neural network offers good approximation for non-linear control methods and is used for trajectory tracking applications[87,118]. Iterative Learning Control (ILC) mechanism is capable of learning the complex fish dynamics and is effective in handling repetitive tasks. It performs speed tracking during entire operation interval rather than asymptotic error convergence in the time domain. It also facilitates improvement in tracking performance amidst partial knowledge of model parameters[109]. In contrast to ILC Repetitive Control (RC) is period based pointwise learning approach, which is not suitable for robotic fish systems because of the control action (frequency, amplitude, and phase) update is possible only at the beginning of each undulatory cycle not during undulation.

Hybridization of multiple controllers has also been evaluated to control robotic fish. Combination of classical PID with a fuzzy controller for Point-To-Point (PTP) locomotion is investigated. In this, PID and fuzzy logic are used for speed and orientation control, respectively. Fuzzy based PID controller uses fuzzy logic to determine the PID control parameters (K_P, K_I, and K_D)[119]. Hybridization of neural network and fuzzy logic with SMC is found to provide optimal tracking control[118,120]. Wen *et al*. investigated that fuzzy based PID controller outperforms in terms of settling time, rising time, steady-state error, and thrust efficiency[121]. Block control mechanism collaborated with feedback lineari-

zation is addressed[122] in aerial vehicles for position control. Block control mechanism divides the multi-variable system into a single-input-single-output system, which simplifies the feedback linearization process. For trajectory tracking in underwater robots, this mechanism can become a potential application and can be further investigated.

7 Analysis of performance parameters

Fish movements can be studied through two ways such as (i) body bound position and (ii) earthbound position. In body bound position, the movement of fish is studied with reference to the central axis of the fish body. It is described by parameters like undulation magnitude, propulsive wavelength, and frequency. This is important to generate the required pattern along the fish body for achieving the desired motion. Unlike body bound position, the earth-bound position is an outcome (navigation) based study. Parameters like speed, distance, acceleration, deceleration, and turning radius are some of the outcomes to evaluate the fish robot performance.

Recent days, most of the robotic fish design focuses on improving these earth-bound parameters, which can increase propulsion speed and enhances maneuverability. To achieve these, efficient mechanical structure and motion control strategies are vital requirements. Design of mechanical structure involves either hyper-redundant discrete body design[123,124] as shown in Fig. 16 or continuous body design[18,110]. The former uses the Multi-Motor Multi-Joint (MMMJ) mechanism and later uses a Single-Motor Multi-Joint (SMMJ) mechanism. The fish robot is discretized into small parts (links L_0, L_1, L_2...L_N) from head to tail, as shown in Fig. 16 to achieve bending motion mimicking a real fish. Here, the links are made up of rigid bodies united by joints. To imitate a real fish movement, the number of joints in the fish robot needs to be increased. These joints may be driven either by a single actuator system or multiple actuators. The latter uses motors (J_1, J_2, ... J_N – active joints) at each joint and can be driven independently but, former uses only one motor to drive the primary joint (J_1 – active joint) and all other secondary joints (J_2, J_3, ... J_N – passive joints) are driven either by wire or translational elements like gears. The MMMJ mechanism produces good propulsion speed and maneuverability at the cost of more electrical

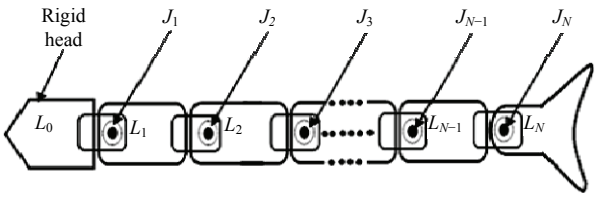

Fig. 16 Multi-joint robotic fish design.

power to drive the actuators. On the other hand, the use of a single motor in SMMJ mechanisms improves energy efficiency[79]. This method is reported to produce lesser propulsion speed, mainly due to rigid links that have to be driven by a single actuator system. Use of flexible links can overcome this problem enabling it to reach higher propulsion speed[3].

Summary of various fish robots currently in existence along with their locomotion parameters reported in the literature are listed in Tables 4 and 5. Observing the effect of undulating or oscillating frequencies on speed of the robot, it is evident that higher speeds are achieved at certain critical frequencies. This frequency is dependent on number of joints participating in the action of undulation or oscillation, body structure, oscillation magnitude, and body-fluid interaction. A sailfish is capable of reaching 110 $km \cdot h^{-1}$ linear velocity, and Pike fish can accelerate as high as 249 $m \cdot s^{-2}$[6], whereas a fish robot can navigate at 13.32 $km \cdot h^{-1}$ (3.7 $m \cdot s^{-1}$)[3].

Comparing turning rates of various robotic fishes given in Table 6, multi-joint fish robot achieves maximum turning rate than single-joint variants. The multi-joint robot can easily generate C-shape movement, which drastically reduces the turning radius and rises turning speed[43]. A peak turning speed of 4500°/s[6] is recorded in archerfish, whereas a fish robot achieves 670°/s with an MMMJ configuration. Realizing a fish robot close to these natural behaviors is still challenging and ongoing research. The performance parameters listed in Tables 4 and 5 is used for the comparison of swimming speeds of different swimming styles of robot fishes. It is grouped into four styles, as discussed in section **2**, such as BCF-oscillation (BCF-O), BCF-undulation (BCF-U), MPF-oscillation (MPF-O), and MPF-undulation (MPF-U). Fig. 17 shows the frequency versus swimming speed plot of various works reported in the literature. For better visualization of performance parameters, logarithmic scale is used in the

Table 4 Typical electrical actuator based robotic fishes and its performance parameters

Reference	Swimming speed		Body length (m)	Frequency (Hz)	Swimming mode	Swimming style	Number of joints	Number of actuators used
	$BL \cdot s^{-1}$	$m \cdot s^{-1}$						
Ref. [125]	0.65	0.3	0.46	0.6	MPF-U	Rajiform	6	6 DC motors
Ref. [126]	0.8	0.4	0.5	1	MPF-U	Rajiform	4	4 Servo motors
Ref. [123]	0.65	0.7	1.08	1	BCF-O	Sub-carangiform	4	4 Servo motors
Ref. [124]	0.8	0.32	0.4	2	BCF-O	Carangiform	4	4 Servo motors
Ref. [16]	1.02	0.2	0.2	0.5	BCF-U	Carangiform	4	4 Servo motors
Ref. [127]	1.15	0.57	0.5	6	BCF-O	Sub-carangiform	4	1 DC motor with 3 passive joints
Ref. [18]	3.4	0.87	0.26	6.6	BCF-O	Carangiform	1	1 (Magnet-based actuator)
Ref. [128]	1.9	0.17	0.09	10	BCF-O	Thunniform	4	4 DC motors
Ref. [43]	1.21	0.53	0.44	2.6	BCF-O	Sub-carangiform	1	1 Servo motor
Ref. [38]	0.7	0.32	0.45	1.4	BCF-O	Sub-carangiform	2	1 Servo motor with one passive joint
Refs. [79,129]	3.07	1.14	0.37	4	BCF-O	Carangiform	2	1 Servo motor with one passive joint
Ref. [3]	11.6	3.7	0.32	20	BCF-O	Carangiform	4	1 Servo motor with 3 passive joints
Ref. [130]	0.5	1.2	2.4	1	BCF-O	Carangiform	1	1 DC motor
Ref. [2]	0.98	0.58	0.59	0.6	BCF-U	Carangiform	4	4 Servo motors
Ref. [131]	1.1	0.32	0.29	4	BCF-O	Carangiform	1	1 Servo motor
Ref. [132]	0.6	0.06	0.1	10	BCF-O	Sub-carangiform	5	5 Magnet-In-Coil Propulsor
Refs. [75,132]	0.85	0.1	0.12	2	BCF-O	Carangiform	2	1 Servo motor with one passive joint
Ref. [17]	4	2	0.5	NA	BCF-O	Sub-carangiform	3	3 Servo motors
Ref. [133]	0.85	0.43	0.5	2	BCF-O	Carangiform	2	2 Servo motors
Ref. [134]	0.25	0.25	0.99	0.6	BCF-U	Anguilliform	10	10 Servomotors
Ref. [135]	0.38	0.42	1.1	1.2	BCF-U	Anguilliform	12	12 DC motors
Ref. [136]	0.52	0.4	0.77	0.4	BCF-U	Anguilliform	7	7 DC motors
Ref. [137]	0.06	0.07	1.19	NA	BCF-U	Anguilliform	9	9 DC motors

NA – Not Available

graph. From the comparison of four swimming styles, the BCF-O style achieved better swimming speed at high frequencies in most of the literature. The BCF-U style also achieved good swimming speed at medium frequencies compared to MPF styles. It is understood that the MPF style locomotion is well suited for special locomotion characteristics like braking, turning, and hovering and not for achieving high-speed swimming.

Locomotion data from Table 4 can be grouped based on single and multiple actuator systems with their swimming speed, as shown in Fig. 18. It is observed that the use of single or multiple actuators for multiple joint systems does not necessarily decide the swimming speed. This is mainly due to the impact of various parameters like frequency, efficient mechanical energy transfer at higher frequencies, streamlined body structure, and stability[3]. Hence, it is important to concentrate on these parameters as well to attain enhanced swimming performance, which is achieved in the literature[17,18] and highlighted in Fig. 18. Recent research work involves usage of an optimization tool for the structural design as it provides the best outcome in terms of thrust. The propulsion parameters, such as flapping frequency and velocity, are directly related to the link lengths and joint angles. Optimization of link lengths and joint angles provide the best fit on traveling wave equation, thus achieving maximum thrust[1,70,148]. The real fish dimensions provide a good base for the development of bio-inspired fish robots. Body length, shape, and mass are the important parameters to mimic a real fish structure. Mass of a real fish is not always constant as it changes based on depth. The body length and shape of the fishes can be utilized as a reference for the design of robot fishes. Some of the real fish body lengths and its swimming speeds presented in Table 7 are taken for the comparison of robot fishes, as shown in Fig. 19.

The comparison of smart actuators-based locomotion, electrical actuator-based locomotion, and natural fish locomotion shown in Fig. 19 concludes that there is a significant gap between smart and electrical actuator

Table 5 Typical smart actuator based robotic fishes and its performance parameters

Reference	Swimming speed		Body length (m)	Frequency (Hz)	Swimming mode	Swimming style	Actuator type	Propulsion part	Max deflection angle
	BL·s^{-1}	m·s^{-1}							
Ref. [57]	0.125	0.02	0.16	2	BCF-O	Carangiform	IPMC	Caudal fin	15
Ref. [58]	0.053	0.0042	0.08	0.4	MPF-U	Rajiform	IPMC	Extended Pectoral fin (Manta ray inspired)	15.5
Ref. [59]	0.067	0.0074	0.11	0.1	MPF-U	Rajiform	IPMC	Extended Pectoral fin (Manta ray inspired)	40
Ref. [52]	0.119	0.021	0.18	1.5	BCF-O	Thunniform	IPMC	Caudal fin	NA
Ref. [46]	0.038	0.05	1.32	0.4	MPF-U	Rajiform	IPMC	Extended Pectoral fin (Manta ray inspired)	NA
Ref. [50]	0.067	0.012	0.18	0.714	BCF-O	Thunniform & Labriform	IPMC	Caudal and two Pectoral fins	NA
Ref. [56]	0.06	0.0078	0.13	1	BCF-O	Carangiform	IPMC	Caudal fin	NA
Ref. [138]	NA	0.0015	NA	0.67	NA	Jet Propulsion	IPMC	Jellyfish inspired	NA
Ref. [53]	0.245	0.024	0.1	2	BCF-U	Carangiform	IPMC	Caudal fin	NA
Ref. [54]	0.034	0.007	0.21	0.157	MPF-U	Rajiform	IPMC	Extended pectoral fins (cownose ray inspired)	10
Ref. [139]	0.092	0.0115	0.13	NA	Oscillation	Turtle inspired	SMA	Chelonia mydas turtle inspired	NA
Ref. [140]	0.905	0.057	0.06	0.4	Oscillation	Jet Propulsion	SMA	Jelly fish inspired	NA
Ref. [141]	0.77	0.112	0.15	2.5	BCF-O	Carangiform	SMA	Caudal fin	NA
Ref. [142]	0.43	0.057	0.13	0.64	MPF-U	Rajiform	SMA	Extended Pectoral fin (Manta ray inspired)	20
Ref. [47]	0.35	0.07	0.2	1	MPF	MPF	SMA	Star fish inspired	NA
Ref. [61]	3.5	0.6	0.17	15	BCF-U	Sub-carangiform	PFC	Entire body	NA
Ref. [143]	0.093	0.0252	0.27	0.9	BCF-O	Thunniform	PFC	Caudal fin	NA
Ref. [64]	0.228	0.04	0.18	5	BCF-O	Thunniform	others	Caudal fin	45
Ref. [64]*	0.138	0.018	0.13	5	BCF-O	Thunniform	others	Caudal fin	45
Ref. [144]	0.77	0.077	0.1	1.5	Oscillation	Leg inspired motion	others	Swimming legs	NA

*Two versions implemented in same paper; NA – Not Available

Table 6 Turning speed of typical robotic fishes

Prototype	Number of joints	Turning speed (°/s)
Ref. [145]	2	33
Ref. [16]	4	120
Ref. [102]	4	120
Ref. [146]	2	38
Ref. [79]	2	90
Ref. [128]	1	14
Ref. [43]	1	12
Ref. [147]	4	670
Ref. [130]	1	75

locomotion as well as a remarkable gap between natural fish and electrical actuator locomotion. This gap is due to the variations in the structure, body length, undulation/oscillation frequency, and actuation principle used for propulsion. Comparing electrical actuators, smart actuators body length and frequency lies in lower range as indicated in Figs. 19 and 20, which results in very low swimming speed.

8 Challenges

This section provides a detailed discussion on challenges in structural design, modeling, and control strategies of fish robots. The research gaps and possible future directions of research in this area are identified and presented below.

Though real fish locomotion inspires many designs in biomimetic fish robot, there still exist significant challenges to be addressed. The maximum swimming speed of swordfish is 27 m·s^{-1}, whereas in robot fish maximum speed of only 3.7 m·s^{-1} have been achieved till date. Similarly, the maximum turning speed of archerfish is 4500°/s[150], whereas a robot fish achieves 670°/s. Additionally, real fish exhibits special behaviors such as a maximum quick start of 249 m·s^{-2} in pike fish, escape maneuvering, braking, and hovering. Achieving these special behaviors in robot fish needs integration of BCF and MPF styles, which encounters synchronization

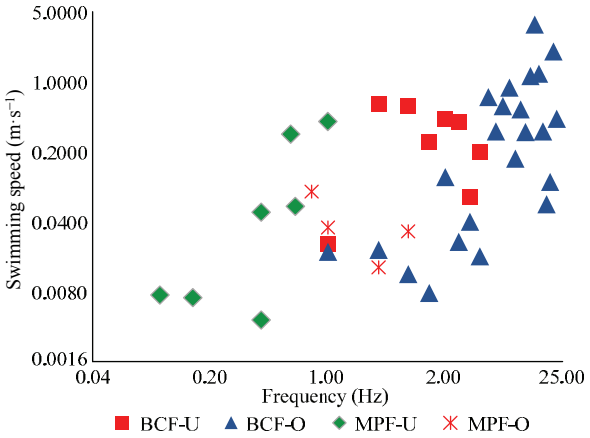

Fig. 17 Comparison of swimming speeds versus frequency using different swimming styles.

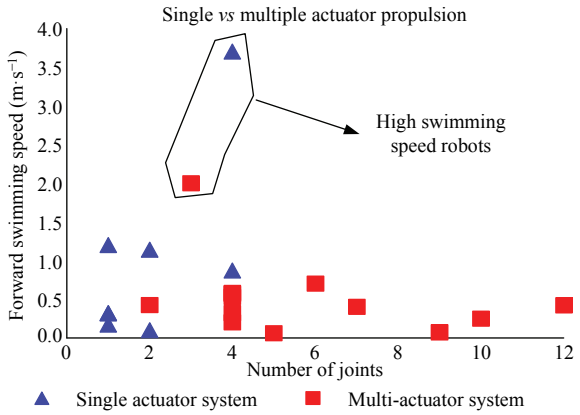

Fig. 18 Single versus multiple actuator systems with respect to the number of joints and swimming speed.

Table 7 Parameters of real fish includes body length and top speed[149]

Name of the fish	Swimming style	Average length (m)	Top speed ($m \cdot s^{-1}$)
European Eel	Anguilliform	0.75	0.8
Giant Moray	Anguilliform	3	2
Sea Snake	Anguilliform	0.63	0.8
Chum Salmon	Sub-carangiform	0.65	5
Chinook Salmon	Sub-carangiform	1	6
Lake Sturgeon	Sub-carangiform	2	1
Swordfish	Carangiform	4.55	27
Bonefish	Carangiform	0.77	17
Giant Trevally	Carangiform	1.7	13
Yellowfin Tuna	Thunniform	1.3	16
Mako Shark	Thunniform	2	13
Bottlenose Dolphin	Thunniform	3	11
Banded Wrasse	Labriform	0.27	0.84
Spotted Wrasse	Labriform	0.158	0.58
Schelegel's Parrotfish	Labriform	0.22	0.85
Box Fish	Ostraciiform	0.13	0.88

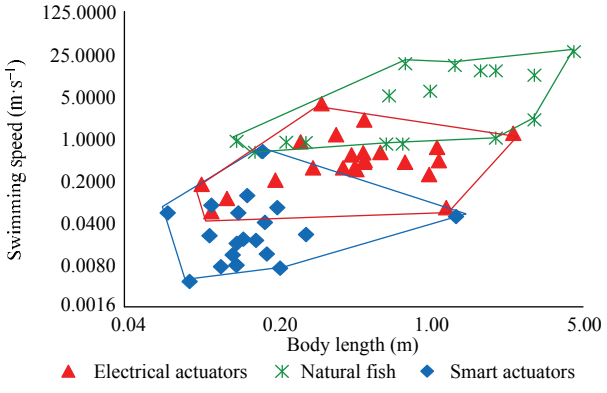

Fig. 19 Swimming speed comparison of biological and artificial fishes with the body length.

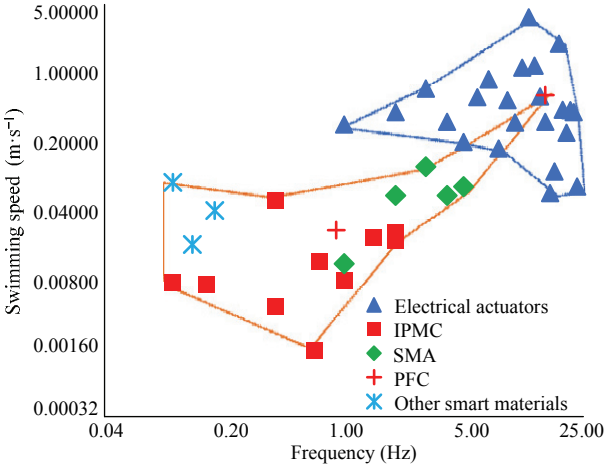

Fig. 20 Comparison of speed versus frequency of robots using different actuators.

problem and design complexity that needs to be addressed by the research community. Optimization algorithms have potential applications in design and control parameters of robot fish. Investigation on use of evolutionary optimization techniques like genetic algorithm, ant colony optimization, particle swarm optimization for robot fish design will be the possible future area of research. The choice of swimming style in robot locomotion plays a vital role in achieving appropriate locomotion characteristics. From literature, thunniform provides energy-efficient locomotion[151], carangiform and sub-carangiform achieve high-speed swimming. Implementation of these styles in real-time applications like underwater exploration, oil, gas leakage inspection, and behavioral study of aquatic lives brings in lot of complexities in stability and buoyancy maintenance demanding precise design.

Apart from rigid bodies, soft bodies structures are

also employed for improving 3D maneuverability of robot fish. Smart and soft actuators are majorly utilized for achieving flexible structures in robot fish. It encounters the problem of poor body stiffness, controlling, and slower response resulting in challenges in terms of material selection, actuator selection, and controller design. Actuator systems with smaller size, lesser weight, and simplified control are preferred to design a fish robot. Smart actuators such as SMA, IPMC, PFC actuators, and soft actuators are used for propulsion in soft robot fishes[47,50,54,110,152]. The IPMC and PFC based smart actuators can generate flapping motion through deformation process, but natural muscle of fish is capable of generating multi-dimensional motion. Therefore, emulation of muscles using IPMC and PFC actuation is a very complex process. Moreover, the interaction studies of soft body with water are challenging as the change in shape of the system is continuous along its body. According to the literature, predominantly flapping frequency for smart actuators is very low (< 5 Hz) as shown in Fig. 20. It limits the smart actuators to achieve high-speed swimming and turning. As a conclusion, the 2-D maneuvering of robot fish using smart actuators provides energy-efficient flapping, but for high speed and 3-D maneuverability, lots of design improvements need to be carried out to reduce actuation time and achieve synchronization.

Dynamic modeling in a non-linear environment and online identification of hydrodynamic parameters like drag force, buoyancy, and thrust force is a promising area to be investigated. Predominantly, Lighthill's EBT, LAEBT models, and Lagrangian models are utilized for the rigid body robot fish modeling, which often encounters linearization problem. Bernoulli-Euler beam equation is utilized for modeling flexible body robot fish, which limits the flapping magnitude. Data-driven modeling can be a potential candidate to overcome the above limitations in conventional techniques. Data-driven models tend to learn about robot fish dynamics using the input and output data, which are collected through trail runs. Offline modeling techniques like neural networks and adaptive neuro-fuzzy inference systems use the data collected from various experiments to encapsulate the robot fish dynamics. However, randomness in the dynamic nature of the medium demands an action-oriented online modeling like reinforcement learning, which could be the possible future direction of research in robot fish modeling.

CPG controller is used to generate gaits in robot fish to mimic real fish locomotion. Due to non-linear load variations or occasional overloading at high-speed, the actuators face the danger of break down or choking, which may lead to undesired pattern formation for swimming. Real-time identification and correction of such faults in the fish robot are essential for autonomous navigation. This situation demands a fault tolerance control mechanism, which monitors the faults continuously and provides control action in accordance. From the literature, it is seen that the implementation of fault tolerance control in robotic fish is sparse[153] and demands further investigation. Predominantly model-based feedback controllers are employed for motion control of non-linear robotic fish. However, the performance of these controllers takes a setback, when they use linearized model for real-time applications. Complexity in precise modeling and non-linear hydrodynamics makes the controller design challenging. Alternatively, intelligent controllers are recently investigated for implementing a model-free design so that it can retain the non-linearity. ILC, fuzzy, neural, and equilibrium-based learning controllers are investigated in literature[24,87,109,118,154], where the convergence of tracking error is significant. These intelligent controllers require prior knowledge about the robot dynamics and their interaction with the underwater environment. Hence, design of these controllers with appropriate knowledge about the robot dynamics can potentially improve the tracking performance. Alternatively, non-linear dynamics of robot fish also encourages the use of adaptive controllers. Implementation of adaptive controllers demands online estimator to track the parametric variation. Limited performance of underwater sensors makes the online estimation of these parametric variations highly challenging. Stochastic filters like Kalman filters, particle filters and their variants can be used to improve the estimation accuracy.

9 Conclusion

A comprehensive review on design, modeling, and control of robotic fish has been presented in this paper.

Based on the review, it is evident that high swimming speed is achieved in BCF type with oscillation mode of locomotion. Structural designs and control strategies for MPF style are investigated widely in literature. However, the performance parameters like swimming speed and maneuverability are not examined thoroughly, which augments the possibility of future research. Use of smart and soft actuators makes the design compact and provides better actuation close to a behavior of real fish muscle. A maximum swimming speed of 0.6 $m \cdot s^{-1}$ is reported in sub-carangiform robot using smart actuators. Hence, selection of actuator plays a major role in robot fish design and has wider scope of research.

Through performance analysis, it was found that maximum swimming speed depends on a critical undulation frequency. This critical frequency depends on the factors like actuation policy, energy transfer mechanism, and body stability. Optimal design of these factors enables to achieve a higher critical frequency and enhances the swimming speed. Hydrodynamic based modeling tools, precise control strategies, and autonomous navigation are some of the important challenges that need significant attention. Machine learning and artificial intelligence tools show outstanding progress in modeling the non-linear dynamics, which encourages their usage in robot fish modeling. Literature shows that adaptive controllers are frequently used for non-linear control applications and can also be extended for fish robots. Here, the major challenge lies in effective sensory feedback, which demands extensive research in the area of sensor development for underwater applications.

References

[1] Koca G O, Korkmaz D, Bal C, Akpolat Z H, Ay M. Implementations of the route planning scenarios for the autonomous robotic fish with the optimized propulsion mechanism. *Measurement*: *Journal of the International Measurement Confederation*, 2016, **93**, 232–242.

[2] Wen L, Liang J H, Wu G H, Li J L. Hydrodynamic experimental investigation on efficient swimming of robotic fish using self-propelled method. *International Journal of Offshore and Polar Engineering*, 2010, **20**, 167–174.

[3] Clapham R J, Hu H S. *iSplash*: Realizing fast Carangiform swimming to outperform a real fish. In Du R, Li Z, Youcef-Toumi K, Valdivia y Alvarado P, eds., *Robot Fish*. *Springer Tracts in Mechanical Engineering*, *Springer*, *Berlin*, *Heidelberg*, 2015, 193–218.

[4] Hu H. Biologically inspired design of autonomous robotic fish at Essex. *Proceedings of the IEEE SMC UK-RI Chapter Conference on Advances in Cybernetic Systems*, Sheffield, England, 2006, 3–8.

[5] Bandyopadhyay P R. Trends in biorobotic autonomous undersea vehicles. *IEEE Journal of Oceanic Engineering*, 2005, **30**, 109–139.

[6] Du R, Li Z, Youcef-Toumi K, Valdivia y Alvarado P. Introduction. In Du R, Li Z, Youcef-Toumi K, Valdivia y Alvarado P, eds., *Robot Fish*. Springer, Berlin, Heidelberg, 2015, 1–24.

[7] Pettigrew J B. *Animal Locomotion*: *Or*, *Walking*, *Swimming*, *and Flying*, *with a Dissertation on Aëronautics*, H S King & Company, New York, USA, 1873.

[8] Breder C. *The Locomotion of Fishes*. Zoologica - Office of the Society, New York, USA, 1926.

[9] Gray J. Studies in animal locomotion: I. The movement of fish with special reference to the eel. *Journal of Experimental Biology*, 1933, **10**, 88–104.

[10] Videler J J. *Fish Swimming*. Chapman and Hall, London, UK, 1993.

[11] Lighthill M J. Hydromechanics of aquatic animal propulsion. *Annual Review of Fluid Mechanics*, 2003, **1,** 413–446.

[12] Lighthill M J. Aquatic animal propulsion of high hydromechanical efficiency. *Journal of Fluid Mechanics*, 1970, **44**, 265–301.

[13] Lighthill M J. Large-amplitude elongated-body theory of fish locomotion. *Proceedings of the Royal Society B*: *Biological Sciences*, London, UK, 1971, 125–138.

[14] Triantafyllou M S, Triantafyllou G S. An efficient-swimming machine. *Scientific American*, 1995, **272**, 64–70.

[15] Liu J D, Hu H S. A 3D simulator for autonomous robotic fish. *International Journal of Automation and Computing*, 2004, **1**, 42–50.

[16] Liu J D, Hu H S. Biological inspiration: From Carangiform fish to multi-joint robotic fish. *Journal of Bionic Engineering*, 2010, **7**, 35–48.

[17] Yang G H, Ryuh Y. Design of high speed fish-like robot "Ichthus V5.7". 10*th International Conference on Ubiquitous Robots and Ambient Intelligence*, Jeju, South Korea, 2013, 451–453.

[18] Clapham R J, Hu H S. iSplash-I: High performance swimming motion of a carangiform robotic fish with full-body coordination. *Proceedings - IEEE International Conference on Robotics and Automation*, Hong Kong, China, 2014, 322–327.

[19] Scaradozzi D, Palmieri G, Costa D, Pinelli A. BCF swimming locomotion for autonomous underwater robots: A review and a novel solution to improve control and efficiency. *Ocean Engineering*, 2017, **130**, 437–453.

[20] Liu H L, Tang Y F, Zhu Q X, Xie G M. Present research situations and future prospects on biomimetic robot fish. *International Journal on Smart Sensing and Intelligent Systems*, 2014, **7**, 458–480.

[21] Bandyopadhyay P R, Beal D N, Menozzi A. Biorobotic insights into how animals swim. *The Journal of Experimental Biology*, 2008, **211**, 206–214.

[22] Colgate J E, Lynch K M. Mechanics and control of swimming: A review. *IEEE Journal of Oceanic Engineering*, 2004, **29**, 660–673.

[23] Raj A, Thakur A. Fish-inspired robots: Design, sensing, actuation, and autonomy - A review of research. *Bioinspiration & Biomimetics*, 2016, **11**, 031001.

[24] Yu J Z, Wang M, Dong H F, Zhang Y L, Wu Z X. Motion control and motion coordination of bionic robotic fish: A review. *Journal of Bionic Engineering*, 2018, **15**, 579–598.

[25] Chu W S, Lee K T, Song S H, Han M W, Lee J Y, Kim H S, Kim M S, Park Y J, Cho K J, Ahn S H. Review of biomimetic underwater robots using smart actuators. *International Journal of Precision Engineering and Manufacturing*, 2012, **13**, 1281–1292.

[26] Faudzi A A M, Razif M R M, Nordin N A M, Natarajan E, Yaakob O. A review on development of robotic fish. *Journal of Transport System Engineering*, 2014, **1**, 12–22.

[27] Xia D, Chen W S, Liu J K, Wu Z. Effect of head swing motion on hydrodynamic performance of fishlike robot propulsion. *Journal of Hydrodynamics*, 2016, **28**, 637–647.

[28] Liu J D, Hu H S. Biologically inspired behaviour design for autonomous robotic fish. *International Journal of Automation and Computing*, 2006, **3**, 336–347.

[29] Sfakiotakis M, Lane D M, Davies J B C. Review of fish swimming modes for aquatic locomotion. *IEEE Journal of Oceanic Engineering*, 1999, **24**, 237–252.

[30] Niu X L, Xu J X, Ren Q Y, Wang Q G. Locomotion learning for an anguilliform robotic fish using central pattern generator approach. *IEEE Transactions on Industrial Electronics*, 2014, **61**, 4780–4787.

[31] Niu X L, Xu J X. Modeling, control and locomotion planning of an Anguilliform robotic fish. *Unmanned Systems*, 2014, **02**, 295–321.

[32] Xu J X, Niu X L. Gait generation and sliding mode control design for anguilliform biomimetic robotic fish. *IECON Proceedings* (*Industrial Electronics Conference*), Melbourne, VIC, Australia, 2011, 3947–3952.

[33] Xu J X, Niu X L, Ren Q Y, Wang Q G. Collision-free motion planning for an Anguilliform robotic fish. *IEEE International Symposium on Industrial Electronics*, Hangzhou, China, 2012, 1268–1273.

[34] Niu X L, Xu J X, Ren QY, Wang Q G. Locomotion generation and motion library design for an Anguilliform robotic fish. *Journal of Bionic Engineering*, 2013, **10**, 251–264.

[35] Suebsaiprom P, Lin C L, Engkaninan A. Undulatory locomotion and effective propulsion for fish-inspired robot. *Control Engineering Practice*, 2017, **58**, 66–77.

[36] Yu J Z, Wu Z X, Wang M, Tan M. CPG network optimization for a biomimetic robotic fish *via* PSO. *IEEE Transactions on Neural Networks and Learning Systems*, 2016, **27**, 1962–1968.

[37] Suebsaiprom P, Lin C L. Maneuverability modeling and trajectory tracking for fish robot. *Control Engineering Practice*, 2015, **45**, 22–36.

[38] Nguyen P L, Lee B R, Ahn K K. Thrust and swimming speed analysis of fish robot with non-uniform flexible tail. *Journal of Bionic Engineering*, 2016, **13**, 73–83.

[39] Kodati P, Hinkle J, Winn A, Deng X Y. Microautonomous robotic ostraciiform (MARCO): Hydrodynamics, design, and fabrication. *IEEE Transactions on Robotics*, 2008, **24**, 105–117.

[40] Peng J, Dabiri J O, Madden P G, Lauder G V. Non-invasive measurement of instantaneous forces during aquatic locomotion: A case study of the bluegill sunfish pectoral fin. *Journal of Experimental Biology*, 2007, **210**, 685–698.

[41] Blake R W. The swimming of the mandarin fish Synchropus picturatus (Callionyiidae: Teleostei). *Journal of the Marine Biological Association of the United Kingdom*, 1979, **59**, 421–428.

[42] Behbahani S B, Tan X. Design and modeling of flexible passive rowing joint for robotic fish pectoral fins. *IEEE Transactions on Robotics*, 2016, **32**, 1119–1132.

[43] Zhang S W, Qian Y, Liao P, Qin F H, Yang J M. Design and control of an agile robotic fish with integrative biomimetic mechanisms. *IEEE/ASME Transactions on Mechatronics*, 2016, **21**, 1846–1857.

[44] Behbahani S B, Tan X B. Role of pectoral fin flexibility in robotic fish performance. *Journal of Nonlinear Science*, 2017, **27**, 1155–1181.

[45] Guo S X, Fukuda T, Asaka K. A new type of fish-like underwater microrobot. *IEEE/ASME Transactions on Mechatronics*, 2003, **8**, 136–141.

[46] Punning A, Anton M, Kruusmaa M. A biologically inspired

ray-like underwater robot with electroactive polymer pectoral fins. *Proceedings of IEEE International Conference on Mechatronics and Robotics*, Aachen, Germany, 2004, 241–245.

[47] Jin H, Dong E B, Alici G, Mao S X, Min X, Liu C S, Low K H, Yang J. A starfish robot based on soft and smart modular structure (SMS) actuated by SMA wires. *Bioinspiration & Biomimetics*, 2016, **11**, 056012.

[48] Wang Z L, Hang G R, Li J A, Wang Y W, Xiao K. A micro-robot fish with embedded SMA wire actuated flexible biomimetic fin. *Sensors and Actuators A*: *Physical*, 2008, **144**, 354–360.

[49] Song S H, Lee J Y, Rodrigue H, Choi I S, Kang Y J, Ahn S H. 35 Hz shape memory alloy actuator with bending-twisting mode. *Scientific Reports*, 2016, **6**, 21118.

[50] Ye Z H, Hou P Q, Chen Z, Member I. 2-D maneuverable robotic fish propelled by multiple ionic polymer–metal composite artificial fins. *International Journal of Intelligent Robotics and Applications*, 2017, **1**, 195–208.

[51] Aureli M, Kopman V, Porfiri M. Free-locomotion of underwater vehicles actuated by ionic polymer metal composites. *IEEE*/*ASME Transactions on Mechatronics*, 2010, **15**, 603–614.

[52] Wang T M, Shen Q, Wen L, Liang J H. On the thrust performance of an ionic polymer-metal composite actuated robotic fish: Modeling and experimental investigation. *Science China Technological Sciences*, 2012, **55**, 3359–3369.

[53] Ye X F, Su Y D, Guo S X, Wang L Q. Design and realization of a remote control centimeter-scale robotic fish. *IEEE*/*ASME International Conference on Advanced Intelligent Mechatronics*, Xi'an, China, 2008, 25–30.

[54] Chen Z, Um T I, Zhu J Z, Bart-Smith H. Bio-inspired robotic cownose ray propelled by electroactive polymer pectoral fin. *Proceedings of the ASME International Mechanical Engineering Congress and Exposition* 2011, 2012, **2**, 817–824.

[55] Kim J, Jeon J H, Kim H J, Lim H, Oh I K. Durable and water-floatable ionic polymer actuator with hydrophobic and asymmetrically laser-scribed reduced graphene oxide paper electrodes. *ACS Nano*, 2014, **8**, 2986–2997.

[56] Aureli M, Kopman V, Porfiri M. Free-locomotion of underwater vehicles actuated by ionic polymer metal composites. *IEEE*/*ASME Transactions on Mechatronics*, 2010, **15**, 603–614.

[57] Chen Z, Shatara S, Tan X B. Modeling of biomimetic robotic fish propelled by an ionic polymer-metal composite caudal fin. *IEEE*/*ASME Transactions on Mechatronics*, 2010, **15**, 448–459.

[58] Chen Z, Um T I, Bart-Smith H. A novel fabrication of ionic polymer-metal composite membrane actuator capable of 3-dimensional kinematic motions. *Sensors and Actuators A*: *Physical*, 2011, **168**, 131–139.

[59] Chen Z, Um T I, Bart-Smith H. Bio-inspired robotic manta ray powered by ionic polymer-metal composite artificial muscles. *International Journal of Smart and Nano Materials*, 2012, **3**, 296–308.

[60] Um T I, Chen Z, Bart-Smith H. A novel electroactive polymer buoyancy control device for bio-inspired underwater vehicles. *IEEE International Conference on Robotics and Automation*, Shanghai, China, 2011, 172–177.

[61] Zhao W J, Ming A G, Shimojo M. Development of high-performance soft robotic fish by numerical coupling analysis. *Applied Bionics and Biomechanics*, 2018, 5697408.

[62] Katzschmann R K, DelPreto J, MacCurdy R, Rus D. Exploration of underwater life with an acoustically controlled soft robotic fish. *Science Robotics*, 2018, **3**, eaar3449.

[63] Tolley M T, Shepherd R F, Mosadegh B, Galloway K C, Wehner M, Karpelson M, Wood R J, Whitesides G M. A resilient, untethered soft robot. *Soft Robotics*, 2014, **1**, 213–223.

[64] Zhang ZG, Yamashita N, Gondo M, Yamamoto A, Higuchi T. Electrostatically actuated robotic fish: Design and control for high-mobility open-loop swimming. *IEEE Transactions on Robotics*, 2008, **24**, 118–129.

[65] Bonnet F, Crot N, Burnier D, Mondada F. Design methods for miniature underwater soft robots. 6*th IEEE International Conference on Biomedical Robotics and Biomechatronics* (*BioRob*), Singapore, 2016, 1365–1370.

[66] Bonnet F, Kato Y, Halloy J, Mondada F. Infiltrating the zebrafish swarm: design, implementation and experimental tests of a miniature robotic fish lure for fish–robot interaction studies. *Artificial Life and Robotics*, 2016, **21**, 239–246.

[67] Takada Y, Araki R, Nakanishi Y, Nonogaki M, Ebita K, Wakisaka T. Development of small fish robots powered by small and ultra-light passive-type polymer electrolyte fuel cells. *Journal of Robotics and Mechatronics*, 2010, **22**, 150–157.

[68] Borazjani I. *Numerical Simulations of Fluid-Structure Interaction Problems in Biological Flows*. [2016-05-18], http://hdl.handle.net/11299/46070.

[69] Videler J J. Interactions between fish and water. *Fish Swimming*, Springer, Dordrecht, 1993, 1–22.

[70] Yu J Z, Yuan J, Wu Z X, Tan M. Data-driven dynamic modeling for a swimming robotic fish. *IEEE Transactions*

on Industrial Electronics, 2016, **63**, 5632–5640.

[71] Fiazza C, Salumäe T, Listak M, Kulikovskis G, Templeton R, Akanyeti O, Megill W, Fiorini P, Kruusmaa M. Biomimetic mechanical design for soft-bodied underwater vehicles. *OCEANS*'10 *IEEE Sydney*, *OCEANSSYD* 2010, Sydney, NSW, Australia, 2010, 1–7.

[72] El Daou H, Salumäe T, Chambers L D, Megill W M, Kruusmaa M. Modelling of a biologically inspired robotic fish driven by compliant parts. *Bioinspiration & Biomimetics*, 2014, **9**, 016010.

[73] Kopman V, Laut J, Acquaviva F, Rizzo A, Porfiri M. Dynamic modeling of a robotic fish propelled by a compliant tail. *IEEE Journal of Oceanic Engineering*, 2015, **40**, 209–221.

[74] Alvarado P V Y, Youcef-Toumi K. Design of machines with compliant bodies for biomimetic locomotion in liquid environments. *Journal of Dynamic Systems*, *Measurement*, *and Control*, 2006, **128**, 3–13.

[75] Kopman V, Porfiri M. Design, modeling, and characterization of a miniature robotic fish for research and education in biomimetics and bioinspiration. *IEEE*/*ASME Transactions on Mechatronics*, 2013, **18**, 471–483.

[76] Meirovitch L. *Fundamentals of Vibrations*. McGraw-Hill, New York, USA, 2001.

[77] Yu J Z, Wang C, Xie G M. Coordination of multiple robotic fish with applications to underwater robot competition. *IEEE Transactions on Industrial Electronics*, 2016, **63**, 1280–1288.

[78] Khatib B S. *Springer Handbook of Robotics*, Springer, Berlin, Heidelberg, 2016.

[79] Yu J Z, Zhang C, Liu L Q. Design and control of a single-motor-actuated robotic fish capable of fast swimming and maneuverability. *IEEE*/*ASME Transactions on Mechatronics*, 2016, **21**, 1711–1719.

[80] Zhong Y, Song J L, Yu H Y, Du R X. Toward a transform method from lighthill fish swimming model to biomimetic robot fish. *IEEE Robotics and Automation Letters*, 2018, **3**, 2632–2639.

[81] Yu J Z, Sun F H, Xu D, Tan M. Embedded vision-guided 3-D tracking control for robotic fish. *IEEE Transactions on Industrial Electronics*, 2016, **63**, 355–363.

[82] Chowdhury A R, Kumar V, Prasad B, Kumar R, Panda S K. Kinematic study and implementation of a bio-inspired robotic fish underwater vehicle in a lighthill mathematical framework. *Robotics and Biomimetics*, 2014, **1**, 15.

[83] Lighthill M J. Note on the swimming of slender fish. *Journal of Fluid Mechanics*, 1960, **9**, 305.

[84] Carling J, Williams T L, Bowtell G. Self-propelled anguilliform swimming: simultaneous solution of the two-dimensional navier-stokes equations and Newton's laws of motion. *Journal of Experimental Biology*, 1998, **201**, 3143–3166.

[85] Kane T R, Levinson D A. The use of Kanes's dynamical equations in robotics. *The International Journal of Robotics Research*, 1983, **2**, 3–21.

[86] Yen W K, Sierra D M, Guo J. Controlling a robotic fish to swim along a wall using hydrodynamic pressure feedback. *IEEE Journal of Oceanic Engineering*, 2018, **43**, 369–380.

[87] Zhou C, Hou Z G, Cao Z, Wang S, Tan M. Motion modeling and neural networks based yaw control of a biomimetic robotic fish. *Information Sciences*, 2013, **237**, 39–48.

[88] Kaihatu J M, Ananthakrishnan P. Mechanics of ocean waves. In Dhanak M R, Xiros N I, eds., *Springer Handbook of Ocean Engineering*, Springer, Cham, 2016, 77–100.

[89] Taylor G. Analysis of the swimming of long and narrow animals. *Proceedings of the Royal Society A*: *Mathematical, Physical and Engineering Sciences*, 1952, **214**, 158–183.

[90] Wu T Y T. Swimming of a waving plate. *Journal of Fluid Mechanics*, 1961, **10**, 321–344.

[91] Wang J, McKinley P K, Tan X. Dynamic modeling of robotic fish with a base-actuated flexible tail. *Journal of Dynamic Systems*, *Measurement*, *and Control*, 2014, **137**, 011004.

[92] Hu T, Low K H, Shen L, Xu X. Effective phase tracking for bioinspired undulations of robotic fish models: A learning control approach. *IEEE*/*ASME Transactions on Mechatronics*, 2014, **19**, 191–200.

[93] Chen X Y, Yu J Z, Wu Z X, Meng Y, Kong S H. Toward a maneuverable miniature robotic fish equipped with a novel magnetic actuator system. *IEEE Transactions on Systems*, *Man*, *and Cybernetics*: *Systems*, 2018, 1–11.

[94] Ljung L. *System Identification* : *Theory for the User*. Prentice Hall, Upper Saddle River, NJ, USA, 1999.

[95] Unbehauen H, Rae G P, Rao G P. A review of identification in continuous-time systems. *Annual Reviews in Control*, 1998, **22**, 145–171.

[96] Saurad V, Xu J X. Analytic modelling for precise speed tracking of multilink robotic fish. *IEEE Transactions on Industrial Electronics*, 2018, **65**, 5665–5672.

[97] Saurad V, Xu J X. Data-assisted modeling and speed control of a robotic fish. *IEEE Transactions on Industrial Electronics,* 2017, **64**, 4150–4157.

[98] Hoang K A, Vo T Q. A study on fuzzy based controllers design for depth control of a 3-joint Carangiform fish robot.

2013 *International Conference on Control*, *Automation and Information Sciences*, Nha Trang, Vietnam, 2013, 289–294.

[99] Suebsaiprom P, Saimek S, Chaisawadi A. Water level control for stabilizing platform. *Proceeding of ECTI Annual Conference*, 2004, 226–229.

[100] Zhou C, Cao Z Q, Wang S, Tan M. The posture control and 3-D locomotion implementation of biomimetic robot fish. *IEEE International Conference on Intelligent Robots and Systems*, Beijing, China, 2006, 5406–5411.

[101] Suebsaiprom P, Lin C L. 2-DOF barycenter mechanism for stabilization of fish-robots. *Proceedings of the* 2013 *IEEE* 8*th Conference on Industrial Electronics and Applications*, Melbourne, VIC, Australia, 2013, 1119–1122.

[102] Yu J Z, Liu L Z, Wang L, Tan M, Xu D. Turning control of a multilink biomimetic robotic fish. *IEEE Transactions on Robotics*, 2008, **24**, 201–206.

[103] Zhao W, Hu Y H, Zhang L, Wang L. Design and CPG-based control of biomimetic robotic fish. *IET Control Theory & Applications*, 2009, **3**, 281–293.

[104] Hu Y H, Liang J H, Wang T M. Parameter synthesis of coupled nonlinear oscillators for CPG-based robotic locomotion. *IEEE Transactions on Industrial Electronics*, 2014, **61**, 6183–6193.

[105] Hu Y H, Tian W C, Liang J H, Wang T M. Learning fish-like swimming with a CPG-based locomotion controller. *IEEE International Conference on Intelligent Robots and Systems*, San Francisco, CA, USA, 2011, 1863–1868.

[106] Yu J Z, Tan M, Chen J, Zhang J W. A survey on CPG-inspired control models and system implementation. *IEEE Transactions on Neural Networks and Learning Systems*, 2014, **25**, 441–456.

[107] Zhao W, Yu J Z, Fang Y M, Wang L. Development of multi-mode biomimetic robotic fish based on central pattern generator. *IEEE International Conference on Intelligent Robots and Systems*, Beijing, China, 2006, 3891–3896.

[108] Phamduy P, Cheong J, Porfiri M. An Autonomous Charging System for a Robotic Fish. *IEEE*/*ASME Transactions on Mechatronics*, 2016, **21**, 2953–2963.

[109] Li X, Ren Q, Xu J X. Precise speed tracking control of a robotic fish via iterative learning control. *IEEE Transactions on Industrial Electronics*, 2016, **63**, 2221–2228.

[110] Marchese A D, Onal C D, Rus D. Autonomous soft robotic fish capable of escape maneuvers using fluidic elastomer sctuators. *Soft Robotics*. 2014, **1**, 75–87.

[111] Chuang M C, Hwang J N, Williams K, Towler R. Tracking live fish from low-contrast and low-frame-rate stereo videos. *IEEE Transactions on Circuits and Systems for Video Technology*, 2015, **25**, 167–179.

[112] Pizarro O, Eustice R M, Singh H. Large area 3-D reconstructions from underwater optical surveys. *IEEE Journal of Oceanic Engineering*, 2009, **34**, 150–169.

[113] Çelebi A T, Ertürk S. Visual enhancement of underwater images using Empirical Mode Decomposition. *Expert Systems with Applications*, 2012, **39**, 800–805.

[114] Schechner Y, Karpel N. Clear underwater vision. *Proceedings of the* 2004 *IEEE Computer Society Conference on Computer Vision and Pattern Recognition*, Washington DC, USA, 2004, 536–543.

[115] Zhang F T, Ennasr O, Litchman E, Tan X B. Autonomous sampling of water columns using gliding robotic fish: Algorithms and harmful-algae-sampling experiments. *IEEE Systems Journal*, 2016, **10**, 1271–1281.

[116] Kato N. Control performance in the horizontal plane of a fish robot with mechanical pectoral fins. *IEEE Journal of Oceanic Engineering*, 2000, **25**, 121–129.

[117] Cao Z Q, Shen F, Zhou C, Gu N, Nahavandi S, Xu D. Heading control for a robotic dolphin based on a self-tuning fuzzy strategy. *International Journal of Advanced Robotic Systems*, 2016, **13**, 28.

[118] Niu Y G, Wang X Y, Hu C. Neural network output feedback control for uncertain robot. *Proceedings of the* 4*th World Congress on Intelligent Control and Automation*, Shanghai, China, 2002, 1980–1984.

[119] Hoang K A, Vo T Q. A study on controllers design based on centroid displacements for depth motion of a 3-joint Carangiform fish robot. In Zelinka I, Duy V, Cha J, eds., *AETA* 2013: *Recent Advances in Electrical Engineering and Related Sciences*. *Lecture Notes in Electrical Engineering*, Springer, Berlin, Heidelberg, 2014, **282**, 545–554.

[120] Zou K X, Wang C, Xie G M, Chu T G, Wang L, Jia Y M. Cooperative control for trajectory tracking of robotic fish. *Proceedings of the American Control Conference*, St. Louis, MO, USA, 2009, 5504–5509.

[121] Wen L, Wang T M, Wu G H, Liang J H, Wang C L. Novel method for the modeling and control investigation of efficient swimming for robotic fish. *IEEE Transactions on Industrial Electronics*, 2012, **59**, 3176–3188.

[122] Tu Duong V, Kim H K, Nguyen T T, Oh S J, Kim S B. Position Control of a Small Scale Quadrotor Using Block Feedback Linearization Control. In Zelinka I, Duy V, Cha J, eds., *AETA* 2013: *Recent Advances in Electrical Engineering and Related Sciences*. *Lecture Notes in Electrical Engineering*, Springer, Berlin, Heidelberg, 2014, **282**, 525–534.

[123] Barrett D S, Triantafyllou M S, Yue D K P, Grosenbaugh M

A, Wolfgang M J. Drag reduction in fish-like locomotion. *Journal of Fluid Mechanics*, 1999, **392**, 183–212.

[124] Yu J Z, Tan M, Wang S, Chen E. Development of a biomimetic robotic fish and its control algorithm. *IEEE Transactions on Systems*, *Man*, *and Cybernetics*, *Part B*: *Cybernetics*, 2004, **34**, 1798–1810.

[125] Cai Y R, Bi S S, Zheng L C. Design optimization of a bionic fish with multi-joint fin rays. *Advanced Robotics*, 2012, **26**, 177–196.

[126] Zhou C L, Low K H. Design and locomotion control of a biomimetic underwater vehicle with fin propulsion. *IEEE*/*ASME Transactions on Mechatronics*, 2012, **17**, 25–35.

[127] Wu Z X, Yu J Z, Tan M, Zhang J W. Kinematic comparison of forward and backward swimming and maneuvering in a self-propelled sub-carangiform robotic fish. *Journal of Bionic Engineering*, 2014, **11**, 199–212.

[128] Chen X Y, Wu Z X, Zhou C, Yu J Z. Design and implementation of a magnetically actuated miniature robotic fish, *IFAC-PapersOnLine*, 2017, **50**, 6851–6856.

[129] Zhang C, Yu J Z, Tan M. Swimming performance of a robotic fish in both straight swimming and making a turn. *IEEE International Conference on Mechatronics and Automation,* Beijing, China, 2015, 1111–1115.

[130] Anderson J M, Chhabra N K. Maneuvering and stability performance of a robotic tuna. *Integrative and Comparative Biology*, 2002, **42**, 118–126.

[131] Alvarado P V Y, Youcef-Toumi K. Modeling and design methodology of an efficient underwater propulsion system. *IASTED International Conference Robotics and Applications*, Salzburg, Austria, 2003, 161–166.

[132] Berlinger F, Dusek J, Gauci M, Nagpal R. Robust maneuverability of a miniature, low-cost underwater robot using multiple fin actuation. *IEEE Robotics and Automation Letters*, 2018, **3**, 140–147.

[133] Ay M, Korkmaz D, Koca G O, Bal C, Akpolat Z H. Mechatronic design and manufacturing of the intelligent robotic fish for bio-inspired swimming modes. *Electronics*, 2018, **7**, 118.

[134] Manfredi L, Assaf T, Mintchev S, Marrazza S, Capantini L, Orofino S, Ascari L, Grillner S, Wallén P, Ekeberg Ö, Stefanini C, Dario P. A boinspired autonomous swimming robot as a tool for studying goal-directed locomotion. *Biological Cybernetics*, 2013, **107**, 513–527.

[135] Crespi A, Karakasiliotis K, Guignard A, Ijspeert A J. Salamandra robotica II: An amphibious robot to study salamander-like swimming and walking gaits. *IEEE Transactions on Robotics*, 2013, **29**, 308–320.

[136] Crespi A, Ijspeert A J. Online optimization of swimming and crawling in an amphibious snake robot. *IEEE Transactions on Robotics*, 2008, **24**, 75–87.

[137] Yu S M, Ma S G, Li B, Wang Y C. An amphibious snake-like robot: Design and motion experiments on ground and in water. *IEEE International Conference on Information and Automation*, Zhuhai, China, 2009, 500–505.

[138] Najem J, Sarles S A, Akle B, Leo D J. Biomimetic jellyfish-inspired underwater vehicle actuated by ionic polymer metal composite actuators. *Smart Materials and Structures*, 2012, **21**, 094026.

[139] Song S H, Kim M S, Rodrigue H, Lee J Y, Shim J E, Kim M C, Chu W S, Ahn S H. Turtle mimetic soft robot with two swimming gaits. *Bioinspiration & Biomimetics*, 2016, **11**, 036010.

[140] Shi L W, Guo S, Asaka K. A novel jellyfish-like biomimetic microrobot. *IEEE*/*ICME International Conference on Complex Medical Engineering*, Gold Coast, QLD, Australia, 2010, 277–281.

[141] Wang Z L, Hang G R, Wang Y W, Li J, Du W. Embedded SMA wire actuated biomimetic fin: A module for biomimetic underwater propulsion. *Smart Materials and Structures*, 2008, **17**, 025039.

[142] Wang Z L, Wang Y W, Li J A, Hang G R. A micro biomimetic manta ray robot fish actuated by SMA. *IEEE International Conference on Robotics and Biomimetics* (*ROBIO*), Guilin, China, 2009, 1809–1813.

[143] Heo S, Wiguna T, Park H C, Goo N S. Effect of an artificial caudal fin on the performance of a biomimetic fish robot propelled by piezoelectric actuators. *Journal of Bionic Engineering*, 2007, **4**, 151–158.

[144] Wang S, Huang B, McCoul D, Li M Y, Mu L L, Zhao J Z. A soft breaststroke-inspired swimming robot actuated by dielectric elastomers. *Smart Materials and Structures*, 2019, **28**, 045006.

[145] Tomie M, Takiguchi A, Honda T, Yamasaki J. Turning performance of fish-type microrobot driven by external magnetic field. *IEEE Transactions on Magnetics*, 2005, **41**, 4015–4017.

[146] Liang J H, Wang T M, Wen L. Development of a two-joint robotic fish for real-world exploration. *Journal of Field Robotics*, 2011, **28**, 70–79.

[147] Su Z S, Yu J Z, Tan M, Zhang J W. Implementing flexible and fast turning maneuvers of a multijoint robotic fish. *IEEE*/*ASME Transactions on Mechatronics*, 2014, **19**, 329–338.

[148] Wang W, Gu D B, Xie G M. Autonomous optimization of swimming gait in a fish robot with multiple onboard sensors. *IEEE Transactions on Systems*, *Man*, *and Cybernetics*: *Systems*, 2019, **49**, 891–903.

[149] Salazar R, Fuentes V, Abdelkefi A. Classification of biological and bioinspired aquatic systems: A review. *Ocean Engineering*, 2018, **148**, 75–114.

[150] Wöhl S, Schuster S. The predictive start of hunting archer fish: A flexible and precise motor pattern performed with the kinematics of an escape C-start. *The Journal of Experimental Biology*, 2007, **210**, 311–324.

[151] Barrett D, Grosenbaugh M, Triantafyllou M. The optimal control of a flexible hull robotic undersea vehicle propelled by an oscillating foil. *Proceedings of Symposium on Autonomous Underwater Vehicle Technology*, Monterey, CA, USA, 1996, 1–9.

[152] Xiang C Q, Guo J L, Chen Y, Hao L N, Davis S. Development of a SMA-Fishing-Line-McKibben Bending Actuator. *IEEE Access*, 2018, **6**, 27183–27189.

[153] Yang Y Q, Wang J, Wu Z J, Yu J Z. Fault-Tolerant Control of a CPG-Governed Robotic Fish. *Engineering*, 2018, **4**, 861–868.

[154] Li X F, Ren Q Y, Xu J X. An equilibrium-based learning approach with application to robotic fish. *Nonlinear Dynamics*, 2018, **94**, 2715–2725.